UNIVERSIDADE DE LISBOA

FACULDADE DE CIÊNCIAS

DEPARTAMENTO DE BIOLOGIA VEGETAL

ΔNp63 is Critical for Progression of High Grade Non-Muscle Invasive Bladder Cancer Through Deregulation of Specific Genetic Pathways

Andreia Filipa Garrido Maia

Mestrado de Biologia Molecular e Genética

Dissertação orientada por:

Doutora Mireia Castillo-Martin

Professora Doutora Rita Maria Pulido Garcia Zilhão

2017

Dedicatória e Agradecimentos

Dedico este trabalho à minha família, especialmente à minha mãe, Lídia Maia, e ao meu pai, Manuel Maia, por toda a educação que me transmitiram, por todos os esforços e sacrifícios e por estarem sempre do meu lado em qualquer circunstância da minha vida. Mostraram-me que ter uma família é ter amor, felicidade, compreensão e sei que devem estar tão orgulhosos de mim como eu deles. Nunca é tarde para lhes agradecer e proveito este momento para o fazer, Obrigada!

Dedico também este trabalho ao meu irmão gémeo, André Maia. Fomos inseparáveis até à faculdade, nascemos, crescemos, brincámos, lutávamos e estudámos sempre juntos. Agora, já adultos vivemos o sucesso um do outro como se fosse o nosso e ambos sabemos que irá ser sempre assim. O seu apoio emocional ajudou-me muito neste percurso.

Dedico este trabalho ao meu namorado e marinheiro, Filipe Dias, por tornar a minha vida muito mais fácil. Agradeço todo o apoio incondicional que me deu em todos os momentos, principalmente nos de incerteza, por todo o amor e paciência e por poder contar com a sua ajuda em qualquer circunstância da minha vida, pessoal e profissional, ainda que tenhamos um oceano entre nós.

Dedico este trabalho aos meus queridos amigos e agradeço-lhes por todo o apoio que me deram não só durante este percurso académico como em todas as ocasiões da minha vida. Agradeço às minhas melhores amigas à Ana Neves, à Inês Bento e à Joana Gameiro por todos estes anos de amizade. Agradeço às minhas amigas da licenciatura à Diana Santos, à Filipa Maia, à Daryna Piontkisvka e à minha afilhada, Inês Vale, pelos momentos felizes que vivemos. Agradeço à Marlene Cabral por todo o apoio que me deu. Agradeço aos amigos que conheci na Fundação Champalimaud, ao Bernardo Esteves, à Carolina Alves, à Magda Negrão, à Mafalda Ferreira e à Sara Correia por tornarem este ano uma experiência inesquecível. Agradeço às amigas que conheci no voleibol e que sei que posso contar com elas para sempre, à Marisa Magalhães e à Joana Silva, mas em especial à Alexandra Oliveira, por todo o tempo que perdeu a ler e corrigir este trabalho, mesmo sem ter tempo nenhum. Agradeço do fundo do coração às minhas queridas colegas de casa, Eva Cunha, Beatriz Correia e Ana Basílio, por todo o apoio emocional, mas principalmente à Eva por todos os conselhos e conhecimentos que me transmitiu.

Este trabalho não seria possível ser a ajuda de várias plataformas e grupos de investigação. Começo por agradecer ao laboratório do Bruno Costa-Silva, System Oncology group, por todo o material e equipamento que partilharam, só assim foi possível começar e terminar este trabalho. Agradeço em especial à Joana Maia não só pela amizade, mas também por todos os conhecimentos que me transmitiu. Agradeço também ao laboratório do Eduardo Moreno, Cell Fitness group, especialmente ao Andrea pela partilha de reagentes e protocolos que permitiram terminar algumas experiências. Agradeço ao laboratório da Rita Fior, Cancer and Telomerases group, pela partilha de linhas celulares, anticorpos e outros materiais de laboratório. Agradeço ao laboratório do Henrique Veiga-Fernandes, Immunophysiology group, por ter partilhado a linha celular HeLa e também a solução de luciferina que permitiu realizar os ensaios *in vivo*, no IMM. Agradeço à 'Flow Cytometry Platform' da Fundação Champalimaud por possibilitar a realização dos ensaios de ciclo celular, agradeço em especial à Ana Vieira por ser tão amável, por me esclarecer todas as minha dúvidas sobre citometria de fluxo e também pela sua amizade. Agradeço à 'Molecular Biology Platform' da Fundação Champalimaud, à Ana Cunha e à Raquel Tomás, por todo o trabalho experimental com o objetivo de produzir e isolar os lentivírus para a inativação do gene *AGR2*. Agradeço à Champalimaud

Advanced BioImaging and BioOptics Experimental Platform' da Fundação Champalimaud por ter possibilitado obter as imagens da imunofluorescência neste trabalho.

Um obrigada muito especial à professora Rita Zilhão, minha orientadora interna na FCUL, por todo o apoio e positivismo. A professora foi incansável em esclarecer a todas as minhas dúvidas que muito ajudaram na realização deste trabalho.

E por último mas não menos importante, agradeço do fundo do coração à Mireia e ao Javier por me terem acolhido tão bem no seu laboratório. Nem mil obrigadas são suficientes para agradecer todos os novos conhecimentos, as novas técnicas e lições de vida que aprendi com eles. Muito obrigada pela paciência, pelas gargalhadas e pela boa disposição. Não foi nada fácil começar este projeto e infelizmente vivemos momentos de grandes angústias e incertezas, no entanto é com grande satisfação que conseguimos juntos terminar este trabalho. Muito obrigada por me terem possibilitado esta experiência e graças a vocês entrego esta tese com muito orgulho no trabalho concluído.

Resumo

Cancro da bexiga é o nono tumor mais comum a nível mundial, com uma estimativa de 429 000 novos casos registados, em 2012, e aproximadamente 165 000 mortes registadas, nesse mesmo ano, em todo o mundo. Os parâmetros clínicos e patológicos usados para avaliar o estádio do cancro da bexiga têm elevadas limitações e até à data ainda não existe nenhum biomarcador que preveja o comportamento tumoral em cada paciente. Por este motivo, é essencial a identificação de novos biomarcadores que estejam envolvidos na progressão tumoral e que permitam reconhecer diferentes tumores de acordo com a sua capacidade progressiva e invasiva. A classificação dos diferentes subtipos de tumor da bexiga permitirá desenvolver um tratamento especializado e individualizado, o que possibilitará uma melhoria da qualidade de vida e da taxa de sobrevivência destes doentes.

O gene *TP63* pertence à família do supressor de tumor *TP53*. No entanto ao contrário do *TP53*, que se encontra mutado em grande parte dos tumores, o gene *TP63* raramente está na sua forma mutada. Ainda assim, a expressão do gene *TP63* está alterada em alguns tumores. A isoforma do gene *TP63*, designada por ΔNp63, tem sido estudada como um possível biomarcador na área da oncologia, pois existem evidências que a relacionam com a progressão do tumor da bexiga não invasivo da camada muscular (NMIBC) para um tumor invasivo da camada muscular (MIBC). Estudos sugerem que esta isoforma inibe a senescência e a apoptose celular assim como promove a tumorogénese, proliferação e sobrevivência celular, exibindo características oncogénicas. No tecido normal da bexiga, o ΔNp63 tem uma alta/elevada expressão enquanto que no tecido tumoral de bexiga esta isoforma encontra-se subregulada.

Este projeto foi iniciado em Mount Sinai, Nova Iorque, pela orientadora deste trabalho, Dr.ª Mireia Castillo, onde, após inativar o gene ΔNp63 das linhas celulares de NMIBC (RT112 e BFTC), observou que estas células apresentavam maior taxa de proliferação *in vitro* e *in vivo*, maior taxa de invasão *in vitro* e maior incidência de tumores primários e formação de metástases *in vivo*. Deste modo, foi necessário validar os resultados na Fundação Champalimaud e verificou-se, através do modelo ortotópico *in vivo*, que as células clones (BFTC_C e RT112_C) apresentaram maior agressividade tumoral e maior formação de metástases, assim confirmando o que tinha sido observado anteriormente. Através da análise da expressão génica, observou-se ainda que ambas as linhas celulares apresentavam nove e quatro genes, respetivamente sobrerregulados e subregulados, concomitantemente nas duas linhas celulares, respetivamente.

Desta forma, o segundo objetivo deste projeto consistiu em descobrir quais dos genes selecionados na análise de expressão génica seriam mais relevantes na progressão tumoral. No entanto, apenas quatro dos nove sobrerregulados (*AGR2, HOXC6, HRK* e *S100A4*) e dois dos quatro genes subregulados (*SCML1* e *SPOCK1*) foram estudados, com base no seu relacionamento com o desenvolvimento tumoral referido na literatura e também por existirem bons anticorpos e *primers* específicos. Deste modo, extraiu-se RNA das quatro linhas celulares (RT112_L_C, RT112_L_P, BFTC_L_C e BFTC_L_P) para realizar ensaios quantitativos de reação em cadeia de polimerase em tempo real (qRT-PCR) de forma a validar os resultados obtidos pela análise da expressão génica. A partir das mesmas linhas celulares foi extraída proteína para realizar ensaios de *western blot* (WB) e ensaios de imunofluorescência (IF), estes últimos foram realizados em células fixadas. Estas técnicas permitiram quantificar os níveis de proteína em cada linha celular (BFTC_P, BFTC_C, RT112_P e RT112_C). Após comparar os níveis de RNA mensageiro (mRNA) e de proteína, *AGR2* foi o gene eleito como um dos favoritos a ter um papel essencial na progressão do tumor da bexiga. *AGR2* tem maior expressão de mRNA nas células clones ($\Delta Np63^{-}$) comparativamente com as

parentais ($\Delta Np63^+$) (observado apenas na linha celular designada BFTC). Relativamente à síntese de proteína, os resultados do WB sugerem que AGR2 é produzida em maior quantidade nas células clones ($\Delta Np63^-$) do que nas parentais ($\Delta Np63^+$) (em ambas as linhas celulares) e através de IF observa-se o mesmo resultado na linha celular BFTC. Outros estudos sugerem que o gene *AGR2* tem funções extracelulares que aumentam a agressividade de diferentes tumores, como por exemplo o cancro do pulmão, da mama e da próstata. Além disso, expressão de mRNA de *AGR2* é elevada no carcinoma de células de transição da bexiga, adenocarcinoma da próstata e do pulmão.

A desativação do gene foi feita em cinco conjuntos de células de cada linha celular de NMIBC, onde já tinha sido inativado a isoforma ΔNp63 do gene *TP63,* formando cinco clones de cada linha celular, designados por BFTC_A1, BFTC_A2, BFTC_A3, BFTC_A4 e BFTC_A5, assim como para a linha celular RT112. Após silenciamento do gene *AGR2* por shRNA nas células BFTC_C e RT112_C, estudaram-se os níveis de mRNA por qRT-PCR, e de proteína através das técnicas de WB e IF para determinar a eficiência da eliminação do mesmo. Estes estudos só foram realizados para a linha celular BFTC. O clone BFTC_A5 mostrou ser o que apresentava menor nível de mRNA e respetiva proteína AGR2, por isso esta linha celular foi utilizada para estudos funcionais, como ensaios de ciclo celular, ensaios de proliferação e ensaios de invasão celular. Os estudos funcionais foram essenciais para observar se o gene *AGR2* está envolvido na progressão celular. Ensaios de ciclo celular revelaram que as células tumorais designadas BFTC_A5 ($\Delta Np63^-$ $AGR2^-$) apresentaram menor divisão celular comparativamente às células tumorais BFTC_C ($\Delta Np63^-$ $AGR2^+$) e BFTC_P ($\Delta Np63^+$ $AGR2^+$), *in vitro*. As células tumorais BFTC_A5 ($\Delta Np63^-$ $AGR2^-$) revelaram ainda menor capacidade de proliferação e de invasão celular, *in vitro*.

Estes estudos sugerem que o gene *AGR2* pode estar envolvido na progressão do tumor da bexiga não invasivo da camada muscular (NMIBC) para invasivo da camada muscular (MIBC). As células tumorais que sintetizam em simultâneo a isoforma ΔNp63 e o gene *AGR2* (BFTC_P) revelaram não ter capacidades tão proliferativas e tão invasoras como as células tumorais que apenas sintetizam AGR2 (BFTC_C). No entanto quando o gene *AGR2* é desligado, estas células tumorais voltam a perder a sua capacidade invasora e proliferativa, sugerindo assim que o gene *AGR2* é essencial para a proliferação e invasão tumoral.

Este trabalho é o primeiro que estuda a interação entre o produto do gene *AGR2* e a isoforma ΔNp63 do gene *TP63* na progressão do tumor da bexiga não invasivo da camada muscular. No entanto mais estudos serão necessários para confirmar esta hipótese, nomeadamente estudos com o modelo ortotópico *in vivo* e também a análise de imunofluorescência de *microarrays* de tumores (TMA) que irá validar os resultados *in vitro*, assim como correlacionar a expressão do *AGR2* com as características do doente (prognóstico, presença de metástases, risco de progressão, entre outros). Além disso, é também necessário realizar os mesmos ensaios, descritos neste trabalho, para a linha celular RT112.

Neste trabalho, *AGR2* é descrito como um potencial fator de progressão de NMIBC para MIBC. O gene *AGR2* é importante para o desenvolvimento do tumor e poderá ser um biomarcador com a capacidade de distinguir tumores que devem sofrer um tratamento mais ou menos invasivo. Como por exemplo, pacientes com tumores de elevado risco de progressão poderão beneficiar de uma cistectomia, enquanto que pacientes com tumores de baixo risco de progressão poderão usufruir de um tratamento menos invasivo e de vigilância médica com alguma regularidade.

A existência de um anticorpo contra a proteína AGR2 pode permitir o desenvolvimento de ensaios clínicos em doentes com NMIBC, de modo a testar a sua efetividade no controlo da progressão destes mesmos tumores.

Palavras-chave: Cancro, Bexiga, NMIBC, ΔNp63, AGR2.

Abstract

ΔNp63, an isoform of *TP63* gene, has been described as an essential marker for Non-Muscle Invasive Bladder Cancer (NMIBC) progression. After knocking down ΔNp63 in NMIBC cell lines, nine and four genes were found up-regulated and down-regulated, respectively, through gene expression analysis, in two different bladder tumor cell lines (RT112 and BFTC). From this set of genes, four up-regulated (*AGR2, HOXC6, HRK* and *S100A4*) and two down-regulated genes (*SCML1* and *SPOCK1*) were chosen for further analysis due to the availability of good antibodies and primers, in order to discover which of those genes are more relevant to bladder cancer progression. With this purpose, total RNA was extracted from BFTC and RT112 cells (both parental and knock down for ΔNp63) to perform quantitative real-time polymerase chain reaction (qRT-PCR) and to validate the gene expression analysis. From the same cell lines, proteins were extracted to performed western blot (WB) analysis and immunofluorescence (IF) assays and the protein and RNA levels were compared. The obtained results suggest that *AGR2* gene was the most related in bladder cancer progression. In addition, mRNA level of *AGR2* was higher in knock down clones than in parental cells (verified only in BFTC cells) and WB results showed that AGR2 protein was also higher in knock down than in parental cells. Similar results were observed by IF assay in BFTC cells. Other studies suggested that AGR2 has extracellular functions that increase aggressiveness of different tumors. Moreover, *AGR2* mRNA expression has been described as high in urinary bladder transitional cell carcinoma, prostate adenocarcinoma and lung carcinoma. To study the effects of that gene in bladder tumor progression, *AGR2* was knocked down in RT112_C and BFTC_C cells which had already been knocked down for ΔNp63 and mRNA and protein level studies were performed again through qRT-PCR, WB and IF techniques. After selection of the cell line with lower level of mRNA and protein AGR2, BFTC_A5, functional studies were performed, such as cell cycle, invasion and proliferation assays. Functional studies showed that BFTC_A5 ($\Delta Np63^{-}$ $AGR2^{-}$) cells displayed lower cell division, lower proliferative and invasive capacities compared with BFTC_C ($\Delta Np63^{-}$ $AGR2^{+}$), which suggest that *AGR2* may has a role in bladder tumor progression.

Key words: Cancer, Bladder, NMIBC, ΔNp63, AGR2.

Table of Contents

List of Figures

List of Tables

Glossary of abbreviations

ΔN: Dominant negative

Abs: Absorbance

AGR2: Anterior gradient 2

AR1D1A: AT-rich interaction domain 1A

ATP: Adenosine triphosphate

BC: Bladder Cancer

BCG: Bacillus Calmette-Guerin

BLI: Bioluminescence Imaging

Bp: Base pair

BSA: Bovine serum albumin

CAPS: Calcyphosine

CD44: Cluster of differentiation 44

CD49: Cluster of differentiation 49

CDKN1A: Cyclin dependent kinase inhibitor 1A

cDNA: Complementary DNA

CHD2: Chromodomain helicase DNA-binding protein 2

CIS: Carcinoma *in Situ*

CK18: Cytokeratin 18

CK20: Cytokeratin 20

DAG-1: Alpha dystroglycan

DAPI: 4',6-Diamidino-2-phenylindole

DBD: DNA binding domain

dH_2O: Distilled water

DMEM: Dulbecco's modified eagle medium

EGFR: Epidermal growth factor receptor

ELF3: ETS-related transcription factor Elf-3

EMEM: Eagle's minimum essential medium

EPDR1: Ependymin related 1

ES: Estrogen

FBS: Fetal Bovine Serum

FGFR3: Fibroblast Growth Factor Receptor 3

GAPDH: Glyceraldehyde-3-phosphate dehydrogenase

GCHFR: GTP cyclohydrolase

GSTM1: Glutathione S-transferase μ

HeLa: Helacyton gartleri

HER 2/3: Receptor tyrosine-protein kinase erbB-2

HG: High grade

HOXC6: Homeobox C6

H-RAS: Harvey rat sarcoma viral oncogene

HRK: Harakiri

HRP: Horseradish peroxidase

IF: Immunofluorescence

IgG: Immunogoblin G

IMM: Molecular Medicine Institute

IVIS: *In vivo* imaging system

KDM6A: Lysine demethylase 6A

KRT14: Keratin 14

KRT5: Keratin 5

LB: Lenox L broth

LG: Low grade

LOH: Loss of heterogeneity

LRRC26: Leucine rich repeat containing 26

MIBC: Muscle invasive bladder cancer

mRNA: Messenger RNA

MSH2: MutS homolog 2

MTS: [3-(4,5-dimethylthiazol-2-yl)-5-(3-carboxymethoxyphenyl)-2-(4-sulfophenyl)-2H-tetrazolium]

MYC: c-Myc binding protein homolog

NAT2: N-acetyltransferase

NEAA: Non-essential amino acids

NMI: Non-muscle invasive

NMIBC: Non-muscle invasive bladder cancer

NOD/SCID: Non-obese diabetic / severe combined immunodeficiency

nVC: Number of viable cells

OD: Oligomerization domain

P: Penicillin

PBS: Phosphate-buffered saline

PDI: Protein disulfide-isomerase

PFA: Paraformaldehyde

PI: Propidium iodide

PI3K: Phosphoinosite-3-kinase

PiK3CA: Phosphatidylinositol-4,5-biphosphate 3-kinase catalytic subunit alpha

PMS: Phenazine methosulfate

PPARG: Peroxisome proliferator – activated receptor gamma

PTEN: Phosphatase and tensin homolog

qRT-PCR: Quantitative real-time polymerase chain reaction

Rab-25: Ras-related protein Rab-25 precursor

RB: Retinoblast

RIPA: Radioimmunoprecipitation assay buffer

Rpm: Rotations per minute

RPMI: Roswell park memorial institute

RT: Room temperature

S: Streptomycin

S100A4: S100 Calcium binding protein A4

SAM: Sterile α motif

SCC: Squamous cell carcinoma

SCML1: Sex comb on midleg-like 1

SD: Standard deviation

SDS: Sodium dodecyl sulfate

SORBS2: Sorbin and SH3 domain containing 2

SOX2: SRY-related HMG-box 2

SPOCK1: Sparc/osteonectin, cwcv and kazal-like domains proteoglycan (testican) 1

SPSS: Statistical package for the social science

SRC: SRC proto-oncogene

STAG2: Stromal antigen 2

TA: Transcriptionally active

TAD: Transactivation domain

TBS: Tris buffered solution

TCC: Transitional Cell Carcinoma

TERT: Telomerase reverse transcriptase

TGS: Tris-Glycine Saline

TMA: Tissue microarray

TP53: Tumor protein 53

TP63: Tumor protein 63

TSC1: Tuberous sclerosis 1

TUR: Transurethral resection

TURBT: Transurethral resection of bladder tumors

UC: Urothelial Carcinoma

WB: Western Blot

1 Introduction

1.1 Bladder Cancer

The bladder is a hollow organ in the pelvis and it is formed by a muscle wall that stretches to accommodate urine and coated by a mucosa named urothelium. The urothelium is a transitional epithelium, which has several layers and it is made up of different types of cells.

Bladder Cancer (BC) is the ninth most common cancer with an estimated of 429 000 new cases occurred in 2012 and approximately 165 000 deaths per year worldwide[1,2]. Europe has the highest incidence rates of BC in the world, with an estimated of 151 200 new cases and 52 400 deaths occurred in 2012[2,3].

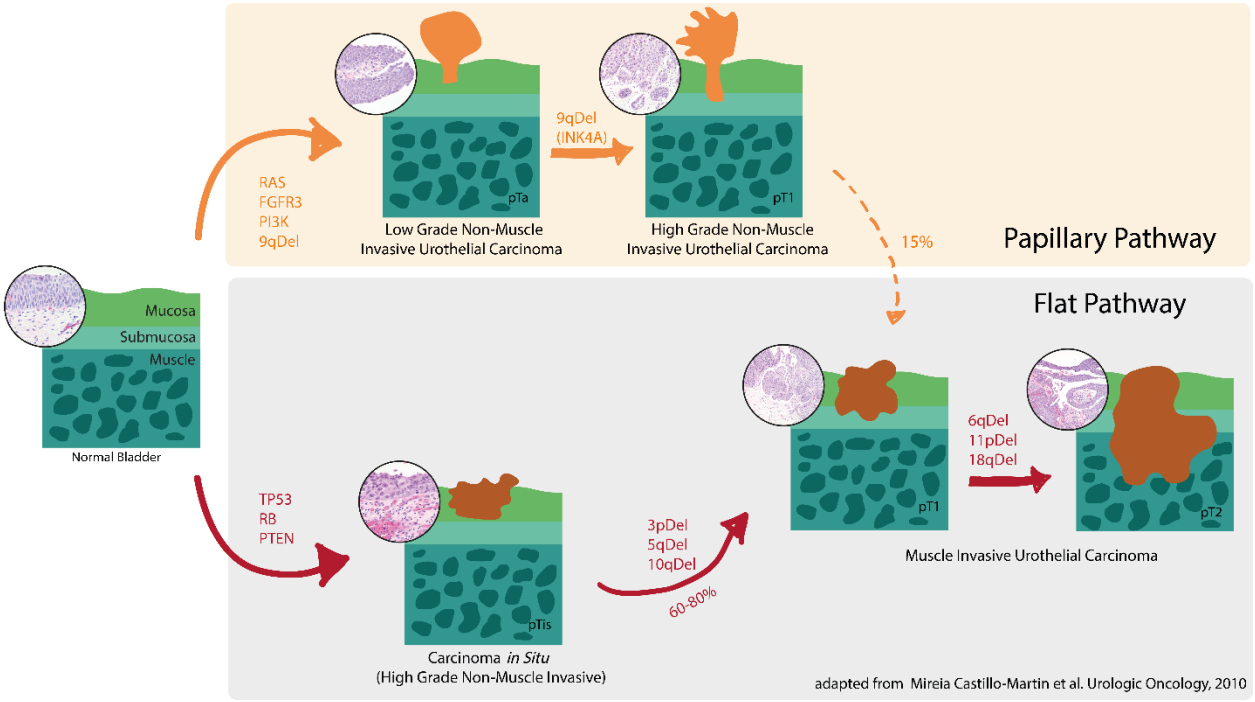

Figure 1.1 Origin and evolution of urothelial carcinoma. Normal bladder is formed by three layers: mucosa layer, submucosa layer and muscle layer. From normal bladder to bladder cancer there are two tumor pathways with divergent genetic backgrounds. Urothelial carcinoma can be low or high grade, depending on the degree of differentiation. Papillary and flat pathways are two distinct tumor morphologies, depending on tumor growth. Bladder cancer can finally be classified as NMIBC, including stages Tis, Ta and T1, or as MIBC, including T2 to T4 stages, depending on invasion of the muscular layer. This figure is adapted from Mireia Castillo-Martin *et al.*[19]**.**

The most common type of BC is urothelial carcinoma (UC) also named transitional cell carcinoma (TCC), because it develops from the transitional epithelium of the bladder[4]. Depending on the depth of invasion through the bladder wall, BC can be classified in two different groups: Non Muscle Invasive Bladder Cancer (NMIBC) and Muscle Invasive Bladder Cancer (MIBC)[5]. NMIBC is also known as superficial BC and is the most frequent group, comprising 75% of the cases at first diagnosis. NMIBC includes stages Tis (also called carcinoma *in situ*, *CIS*), Ta and T1, which have not grown into the muscle layer of the bladder wall, whereas MIBC includes stages T2 to T4 which have invaded the muscle layer of the bladder or further (**Figure 1.1**). Patients with NMIBC have higher chance of survival, around 88-98%

after 5 years, although also a higher chance of recurrence, around 60%, when compared to MIBC[5,6]. Depending on the differentiation degree, BC can be divided in low grade (LG) and high grade (HG), with LG tumors having propensity for recurrence and a good prognosis whereas high grade tumors progress faster and have a worse prognosis. Approximately, 20% of HG NMIBC progress to an invasive and very aggressive tumors[7].

Urothelial carcinoma arises through two distinct molecular pathways with specific histological features, referred as papillary, occurring in 80% of the cases, and non-papillary pathways, occurring in 20%[8,9] (**Figure 1.1**). Papillary carcinomas grow in finger-like projections from the inner surface of the bladder, usually without invading into deeper bladder layers, called also non-muscle invasive (NMI) papillary tumors. These tumors have a high tendency for recurrence but rarely invade the bladder wall or metastasize. On the other hand, non-papillary tumors can evolve from CIS and they can be aggressive enough to invade the bladder wall and to metastasize. LG papillary tumors can progress to HG NMI tumors, typically by the presence of CIS in the adjacent mucosa[8]. Likewise, T1 HG tumors (that invade the lamina propria but do not invade the muscular layer) are associated with high risk of progression, metastasization and death, depending on the depth of invasion of the lamina propria and in the presence of CIS[10]. CIS is a flat HG NMI lesion that can progress to MIBC in 35% to 55% of the cases in 5 years, representing the cause of death in 39% of the patients with BC[11,12]. Some epithelial tumors progress by successive mutations in crucial genes that are responsible for growth regulation, survival, apoptosis and cell-cell interactions[13]. These two distinct pathways of BC have different genetics characteristics: LG NMI papillary tumors are characterized by loss of heterogeneity (LOH) of chromosome 9 and by mutations in harvey rat sarcoma viral oncogene (*H-RAS*), in fibroblast growth factor receptor 3 (*FGFR3*) and in phosphoinosite-3-kinase (*PI3K*) genes, while CIS has structural and functional defects in the *TP53, RB* tumor-suppressor pathways and in phosphatase and tensin homolog *(PTEN*) gene[14–18]. Complete loss of *TP53* gene has been shown to be involved in the development of CIS, and *TP53* loss concomitant with loss of *RB* functions can induce tumor progression[19]. MIBC is characterized by extended genomic aberrations, including LOH of chromosome 3, 5, 6, 10, 11 and 18[20–24].

Due to the discovery of different molecular backgrounds in BC, MIBC was recently classified in molecular subtypes[25]. Luminal tumors are enriched with uroplakins, CK20 and CK18 and have upregulation of peroxisome proliferator – activated receptor gamma (*PPARG*), all characteristic of intermediate/superficial layers of normal urothelium. Luminal tumors express E-cadherin, *HER2/3*, *RAB*-25 and *SRC* and have enrichment of *FGFR3*, *ELF3*, *CDKN1A* and *TSC1* mutations. On the other hand, basal tumors are enriched with expressions of KRT5, KRT14 and CD44 and show up-regulation of *TP63* target genes, *TP53* and *RB1* mutations and show overexpression of CD49, Cyclin B1 and EGFR, similar to cells in the basal layer of normal urothelium[9,26]. Luminal tumors have shown a better prognostic than basal cancers.

Other histological types of cancer can develop in the bladder, including squamous cell carcinoma (SCC, 5 % of the tumors), adenocarcinoma (<1 %), and sarcomas (extremely rare), amongst others.

1.2 Risk Factors

BC is mostly caused by exposure to carcinogenic chemical agents. Tobacco, whether be active or passive smoking, is the leading risk factor for BC, mainly due to exposure to chemical carcinogens such as 4-aminobiphenyl and o-toluidine. Active smokers have 4-fold higher risk of BC incidence, similar to people who started smoking at a younger age or that were exposed to tobacco smoke during childhood[27,28].

Occupational exposure to aromatic amines is another risk factor, for example, exposure to 2-naphthylamine, 4-aminobiphenyl and benzidine and exposure to 4,4'-methylenebis in the dye and rubber industries as well as exposure to hair dyes, house paints, fungicides, ionizing radiation, plastics and others agents can induce BC in 10-15 %[9,29]. Exposure to arsenic and chlorination by products in drinking water represents another group of important risk factors[30]. Chlorine is used to disinfect drinking water and swimming pools and it can dissociate itself in trihalomethanes and when it is present in drinking water can increase the risk of BC. The treatment by radiation of nearby cancers, such as prostate cancer, has also been reported to induce BC. Some other medical conditions may rise the risk of BC, such as the treatment of diabetic patients with pioglitazone drug for more than 2 years[31]. People with bladder infections or who suffer from chronic bladder infections have also more risk of BC. For example, bladder infection by the *Schistosoma* parasite can induce chronic irritation and inflammation in the urinary bladder, presenting higher incidence of squamous cell carcinoma[32].

Family history of BC is also associated with an increased risk for BC mainly resulting of the shared smoking habits. However, some genes have been associated with increased risk of BC such as N-acetyltransferase 2 (*NAT2*) and slow acetylator and glutathione S-transferase μ (*GSTM1*) because their mutated form cannot break some toxins which will accumulate in the bladder[9,33]. *MSH2* mutation found in Lynch syndrome is also associated with a 4.2-fold risk increase for BC in men before the age of 70[33]. Similarly, people with Cowden disease, caused by mutations in *PTEN* gene, have higher risk of developing BC. Despite that, BC consequent of family history is extremely rare[34].

Interestingly, bladder cancer affects men and women in different ways. While men present a considerable higher risk of developing UC of the bladder, women show more advanced disease stages and seem to experience more unfavorable outcomes[35].

1.3 TP63 and Bladder Cancer

TP63, a member of the *TP53* gene family, has been reported as a potential marker of bladder tumor progression[36,37]. *TP63* regulates cell-cycle arrest and apoptosis and encodes two isoforms depending on different promoter use: transcriptionally active (TA) p63 and dominant negative (ΔN) p63 (**Figure 1.2**) [38]. Both TAp63 and ΔNp63 are composed by three isoforms, named α, β and γ depending on alternative splicing.

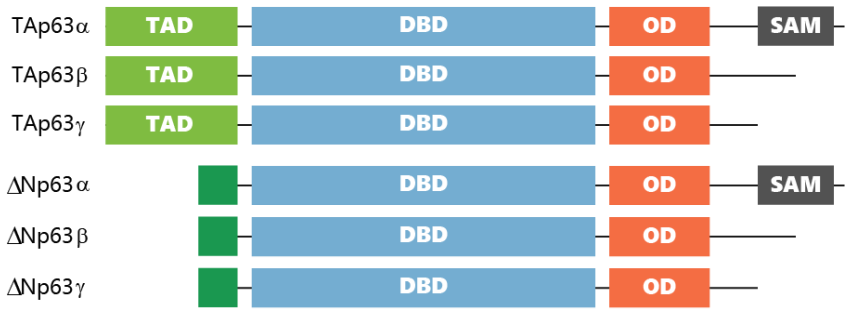

Figure 1.2 p63: protein domain structure. Schematic diagram of p63 isoforms showing the transactivation domain (TAD), DNA binding domain (DBD), oligomerization domain (OD) and sterile α motif (SAM).

In cancer, *TP63* activity is thought to be isoform-specific, with ΔNp63 isoform apparently having an oncogenic role and TAp63 possessing tumor suppressor functions. The TAp63 isoform induces cell cycle

arrest and apoptosis by transactivation of *TP53* whereas ΔNp63 isoform plays a role in blocking transactivation of both *TP53* and TAp63 isoforms of *TP63*. Unlike *TP53*, mutation of the *TP63* gene is very rare in cancer, instead, it is silenced by epigenetic factors[39]. ΔNp63 shows increased expression levels in tumor cells while TAp63 expression levels decrease[40,41]. Therefore, in normal tissue, the detection of ΔNp63 expression is very low, whereas the expression of TAp63 is normal, suggesting that ΔNp63 can be an proto-oncogene[38,39,42]. Even more, previous studies have shown that the same isoform can have different clinical implications in NMIBC and MIBC[43]. Due to these conflicting results, currently there is no consensus about *TP63* being a proto-oncogene or a tumor suppressor, because the different isoforms seem to have opposite effects[41,44,45]. Gaya *et al*. reported that ΔNp63 expression is a marker of good prognosis in HG-NMIBC, since patients whose tumors express this biomarker do not suffer disease progression to MIBC, and subsequently, they do not die from the disease[36].

1.4 Treatment of Bladder Cancer

Treatment of BC depends on the clinical stage and grade at presentation: MIBC needs to be radically treated either by radical cystectomy or systemic therapies or both combined. NMIBC may be removed by trans-urethral resection (TUR) and followed-up to avoid or early detect progression to MIBC. Half of the patients with NMIBC, who are treated with TUR, suffer disease recurrence, and 5-25% of these patients progress to MIBC after repeated recurrences[46]. After TUR, LG Ta tumors are treated with intravesical chemotherapy with Mitomycin C or bacillus Calmette-Guerin (BCG) treatment for 1 year while T1 tumors usually undergo a second TUR followed by BCG treatment for 1 to 3 years[47,48]. On the other hand, high grade NMIBC patients are treated with BCG treatment or intravesical chemotherapy and close follow-up[49]. T1 tumors with high-risk of progression determined by clinical and pathological parameters (including size, multiplicity, localization, associated CIS, prostatic urethra involvement and female gender) may be treated upfront with radical cystectomy to avoid early progression to MIBC, which sometimes may result in an overtreatment[50].

1.5 Biomarkers to Guide BC Clinical Management

NMIBC and MIBC have distinct pathways in carcinogenesis as illustrated in **Figure 1.1** above. One pathway involves mutation of *FGFR3* which is thought to be involved in tumor recurrence[51,52]. This mutation is more frequent in patients with NMIBC than in patients with MIBC at the time of diagnosis but *FGFR3* mutation has not been recognized to be a prognostic biomarker in advanced BC. In contrast, MIBC and CIS exhibit deletions and mutations of *TP53, RB1* or *PTEN. TP53* has a role in induction of apoptosis, inhibition of cell proliferation and arrest of the cell cycle. Nuclear accumulation of p53, which is a poor prognostic factor, is found in 53% of patients who underwent cystectomy in MIBC[53,54]. The *RB1*, a tumor suppressor gene, is a negative regulator of the cell cycle. Loss of *RB1* expression is an adverse prognostic biomarker in MIBC[53]. Bladder cancer with mutation of the *RB1* gene exhibit low *FGFR3* levels and it is associated with significantly poor disease-specific survival[55]. Pietzak *et al.* identified genetic alterations with potential clinical implications in NMIBC[56]. The most frequently altered genes in NMIBC were the *TERT* promoter (73 %), *FGFR3* (49 %), *KDM6A* (38 %), *PIK3CA* (26 %), *STAG2* (23 %), *ARID1A* (21 %) and *TP53* (21 %)[56,57].

Several markers associated with genetic alterations have been identified both in NMIBC and MIBC. Unfortunately, the clinical and pathological parameters have limited prognostic ability and to date no biomarker has been able to predict tumor behavior in an individual patient. Therefore it is important to identify new biomarkers involved in bladder cancer progression that can help clinicians provide individualized risk-stratified decision-making to define which NMIBC patients should be treated with immediate radical cystectomy[58].

Functional studies by our group revealed higher proliferation rate both *in vitro* and *in vivo* as well as increased colony formation activity after knocking down ΔNp63 in NMIBC cells (data not published). Furthermore, these cells displayed superior invasion capacity *in vitro*, which correlated with higher local tumor initiation and metastatic potential in an *in vivo* bladder orthotopic mouse model. Gene expression analyses revealed that there were nine (*AGR2, CAPS, CHD2, GCHFR, HOXC6, HRK, LRRC26, SORBS2* and *S100A4*) and four (*EPDR1, PPARG, SCML1* and *SPOCK1*) commonly up-regulated and down-regulated genes, amongst the experimental cell lines.

Bearing in mind that ΔNp63 isoform could be involved in bladder tumor progression, this work focused in studying the genetic modifications associated with this ΔN isoform loss concomitant with more aggressive tumors.

2 Working Hypothesis and Goals

Considering the relevant role of ΔNp63 in progression of HG NMIBC to MIBC, the main goal of this work is to discover the genetic alterations associated with this TP63 isoform loss that confer the aggressive phenotype to tumor cells. The hypothesis being tested here is that, amongst the differentially regulated genes, *AGR2* may be key in this transformation. To fulfill this final goal, the following objectives will be pursed, by using several *in vitro* and *in vivo* models:

1. Validation of the results obtained by the gene expression arrays for the different genes by qRT-PCR and protein assays (WB and IF).
2. Knocking-down *AGR2* in NMIBC cells using shRNA technology and validation of the downregulation of the gene.
3. Perform cell cycle, proliferation and invasion *in vitro* assays to determine the effect of *AGR2* knock-down in NMIBC cells.

This knowledge will allow a better understanding of the mechanisms of BC progression and in the future, it could help determine how patients with HG NMIBC should be treated, depending on their tumor molecular characteristics as a complement to tumor clinico-pathological features.

3 Material and Methods

3.1 Cell Culture

Two different HG NMIBC commercially available cell lines, RT112 and BFTC, were used for the experiments. These cells came from Dr. Cordon-Cardo's Laboratory at the Icahn School of Medicine at Mount Sinai (New York, USA). First, both lines were transfected with the firefly luciferase gene, and were named RT112_L_P and BFTC_L_P (parental). Then, clones with downregulation of ΔNp63 gene by shRNA technology were generated, called RT112_L_C and BFTC_L_C (**Figure 3.1**). These steps were performed previous to the start of this master project. For this project, *AGR2* was knocked down by shRNA technology in the cells previously ΔNp63 knock down. RT112 cells were grown and maintained in RPMI medium (Lonza #BE12-702F) supplemented with 10 % fetal bovine serum (FBS, Biowest #S181BH-500) and 1 % Penicillin/Streptomycin (P/S, Gibco #15140-122) at 37 °C in a humidified atmosphere of 5 % CO_2. BFTC cells were grown and maintained in DMEM medium (Lonza #BE12-604F) supplemented with 10 % FBS and 1 % P/S at 37 °C in humidified atmosphere of 5 % CO_2.

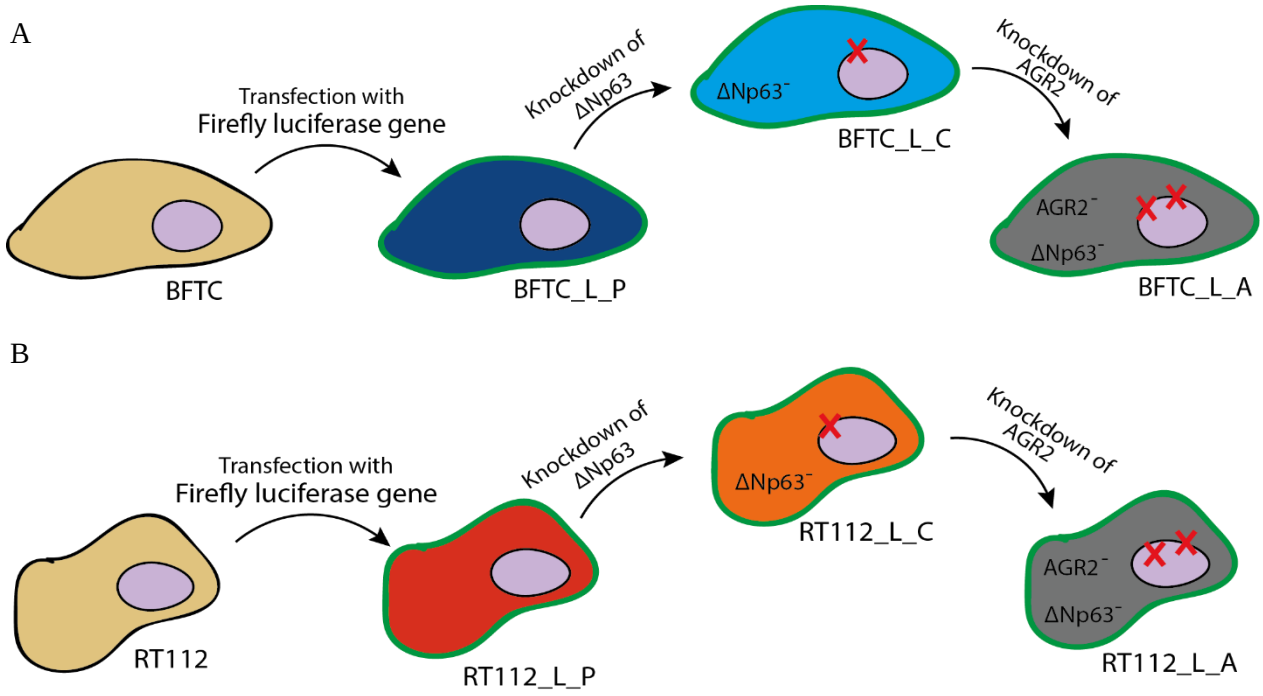

Figure 3.1 Schematic figure of the NMIBC cell lines used in this work. **A:** BFTC cell line (yellow cytoplasm) was transformed with a firefly luciferase gene that conferred bioluminescence signal to the cells (L). These cells were called BFTC_L_P (dark blue cytoplasm) because the only alteration that they have is the luciferase gene. BFTC_L_P cells suffered a knockdown of ΔNp63 gene and were called BFTC_L_C (lighter blue cytoplasm). Then, BFTC_L_C were knockdown for AGR2 gene and were called BFTC_L_A (grey cytoplasm). All of BFTC cell lines studied in this work have the luciferase gene (green membrane). **B:** RT112 cell line (yellow cytoplasm) was transformed with a firefly luciferase gene that conferred bioluminescence signal to the cells (L). These cells were called RT112_L_P (red cytoplasm) because the only alteration that they have is the luciferase gene. RT112_L_P cells suffered a knockdown of ΔNp63 isoform and were called RT112_L_C (orange cytoplasm). Then, RT112_L_C were knockdown for *AGR2* gene and were called RT112_L_A (grey cytoplasm). All of RT112 cell lines studied in this work have the luciferase gene (green membrane).

Human cancer cell line HeLa and MCF-7 were offered by Henrique Veiga-Fernandes Laboratory, IMM (Lisbon, PT) and by the Cancer and Telomere's Laboratory, Champalimaud Foundation (Lisbon, PT), respectively. MCF-7 cells were grown and maintained in the same conditions as BFTC cells and HeLa cells

were grown and maintained in EMEM medium (SIGMA #M2279) supplemented with 10 % FBS, 1 % P/S, 1 % non-essential amino acids (NEAA, Sigma-Aldrich #M7145) and 2 mM L-Glutamine (Biowest #X0551-100) at 37 °C in a humidified atmosphere of 5 % CO_2.

3.2 RNA Extraction and quantitative Real Time PCR

Total RNA was extracted from cultured cells using the RNeasy Mini Kit (Qiagen #74104) following manufacturer's protocol, and concentration and quality assessment was measured using Nanodrop™ 2000 platform. 1µg of mRNA for each cell line (BFTC_L_P, RT112_L_P, BFTC_L_C and RT112_L_C) was converted into cDNA using SuperScript III First-Strand Synthesis kit (Invitrogen #18080-051) according to manufacturer's instructions. The concentration of SuperScript III Reverse Transcriptase used was 100 U/µL.

Quantitative real-time PCR assay allowed to measure the mRNA level in each cell line. This technique with Power SYBR Green PCR Master Mix (Applied Biosystems #4367659) was performed according to the manufacturer's instructions using Biorad CFX96 instrument (Bio-Rad). The sequences of all forward and reverse primers used to analyze the genes of interest (Invitrogen) are summarized in **Table 8.1** (supplementary data). The PCR conditions were: initial denaturation at 95 °C for 15 minutes, 40 cycles of denaturation at 94 °C for 30 seconds, annealing at 60 °C for 40 seconds and elongation at 72 °C for 30 seconds, finishing at 4 °C. GAPDH gene was used as an endogenous control. Analysis was performed by using Bio-Rad CFX Manager software program (Bio-Rad). Relative fold change of target genes was calculated by$2^{-\Delta\Delta Ct}$, where (**Equation 3.1**):

Equation 3.1:

$$- \Delta\Delta Ct = - [\Delta Ct_{clones}(\text{target-GAPDH}) - \Delta Ct_{Parental}(\text{target-GAPDH})]$$

The normalization was defined to the relative expression detected as 1. For each reaction, melting curve analysis was performed to ensure presence of a single amplicon. Experiments were run in triplicates.

3.3 Immunofluorescence Assay

Immunofluorescence (IF) assay allowed quantifying and verifying the subcellular localization of the protein. IF staining was performed on fixed cells. First, coverslips were sterilized in 95 % of ethanol for 10 minutes and then one coverslip was placed in a well of a 6-well plate and let dry. Meanwhile, cells were trypsinized and 100 000 cells were added in each well with the corresponding culture medium (completed up to 2 mL of medium per well). Once they reached 80 % confluency, cells were washed with 1X phosphate-buffered saline (PBS) and fixed with cold 100 % methanol for 15 minutes at -20 °C followed by cold 100 % acetone for 2 minutes at -20 °C. Fixed cells were washed for three times with 1X PBS at room temperature (RT), and kept in 1X PBS at 4 °C until used for staining.

After fixation, cells were permeabilized with 1 % Triton X-100 / 1X PBS at RT for 5 minutes. Then coverslips were incubated with blocking solution (0,1 % Triton X-100 / 1 % bovine serum albumin (BSA) / 1X PBS) at RT for 1h in a wet chamber. After aspiration of blocking solution, primary antibody was incubated for 2h at RT and then rinsed with 1X PBS at RT for 3 minutes, three times. Then, secondary antibody was added at a 1:600 dilution at RT for 45 minutes and then washed with 1X PBS for 3 minutes,

three times. Finally, a drop of mounting medium with DAPI (Thermo Fisher #P36962) was placed on top of the coverslip and it was mounted on a slide. Primary antibodies are summarized in **Table 8.2** (supplementary data). For secondary antibodies, anti-rabbit Alexa 594 (Thermo Fisher #Z25307) and anti-mouse Alexa 594 (Thermo Fisher #Z25007) were used. Slides were put in the dark at -20°C for 20 minutes and then pictures were taken in the Zeiss AxioImager M2, in the Champalimaud Advanced BioImaging and BioOptics Experimental Platform at the Champalimaud Foundation, with 20x amplification. The quantification of the immunofluorescence was measured with a score that related the percentage area of red signal obtained by ImageJ® and the number of nucleus calculated with a semi-automatic software, QuPath.

3.4 Western Blot

3.4.1 Protein Extraction and Quantification

Western blot (WB) is a technique that allows protein quantification and the first step was protein extraction, where Lysis buffer (RIPA buffer, Thermo Fisher #89900) was used, with anti-protease and anti-phosphorylase reagents (Thermo Fisher #A32961), to avoid protein degradation and dephosphorylation. Lysis buffer was mixed with cell pellets and placed on ice (4 °C) for 30 minutes, being vortexed every 10 minutes. Afterwards, solutions were centrifuged at 14000 rpm for 10 minutes at 4°C and the supernatant was recovered and quantified. Protein solution was stored at -80 °C for further immunoblot procedures.

Bradford Law was the baseline to measure protein concentration using the Biorad Solution Protein Assay (Biorad #500-0006), following the manufacturer's instructions. The standard curve was performed with BSA solution at different concentrations, in duplicates. dH_2O was used as a blank. Before measuring the absorbance of the protein solution, 800 µL of dH_2O, 1 µL of the sample and 200 µL of Biorad Solution were put inside of the spectrometry's cuvette, in this particular order. After mixing the solution, it was incubated in the dark at RT for 5 minutes, and finally, the protein solution was read at 595 nm in the Ultrospec 2100 pro (Amersham Bioscience).

3.4.2 Protein Running and Transference

We used 50 µg of protein were used in a total volume of 30 µL for each blot. 4X Laemni dye (Bio-Rad #161-0747) was added to the protein extract. The volume calculations are summarized in **Table 8.3** (supplementary data). Samples were boiled at 95°C for 5 minutes and later kept on ice until gel loading. The running box was prepared with 4-20% Mini-Protean® TGX™ Gels (Bio-Rad #456-1093) and running buffer (Tris-Glycine SDS (TGS) buffer) (Fisher Bioreagents #BP13414). Then, gel was loaded with 5 µL Prestained Rec Protein Ladder (Fisher Bioreagents #161-0374) and 20 µL of each sample. The run was performed at 80-100 V until the dye of the last ladder was at the very bottom of the gel.

For transference of proteins to the membrane, semi-dry transfer technology was used. Foremost, the membrane and two pieces of filter paper in transfer buffer were cut and soaked in a solution, which includes 5,82 g/L of Tris Base (Fisher Bioreagents #BP152-500), 2,93 g/L of Glycine (Fisher Bioreagents #BP381-500), 0,375 g/L of SDS (Fisher Bioreagents #BP166-100), 200 mL of methanol (Acros Organics #423950010) and dH_2O up to 1 L. To do the transfer, 1 wet filter paper was placed on the transfer equipment, and then the wet membrane on top, without bubbles. The gel was placed on top of the membrane, followed by the other wet filter paper and the machine was closed. The running was performed for 60-80 minutes with constant amperage (it was important that the voltage did not surpass 18 V). When the run stopped, the

Ponceau Red (Alfa Aesar #J63139) staining was used to check for visible bands in the membrane corresponding to the different molecular weight proteins.

3.4.3 Immunoblotting

Foremost, the membrane was blocked with 5% non-fat milk (5 g of milk (Bio-Rad #170-6404) in 100 mL of 1X PBS on a rocker for 90 minutes at RT. Primary antibody was prepared in 5% non-fat milk solution and put on the membrane overnight at 4°C, in a rocker. The membrane was rinsed three times, for 30 minutes, in 1X Tris-buffered saline (TBS, Thermo Scientific #28358). The secondary antibody was prepared in 5% non-fat milk solution and put on the membrane for 2 hours at RT. The membrane was washed three times for 30 minutes in 1X TBS. Developing solution Pierce ECL Plus Western (Thermo Fisher #32132) was prepared and placed on top of the membrane for 5 minutes, and imaged in the Amersham™ Imager 600 machine (GE Healthcare Life Science). The same procedure with the loading control protein, β-actin, was performed in the original membrane to determine homogeneous protein load. However, to study S100A4 protein expression, the membrane was blocked with a different blocking solution, BSA blocking solution (5 % BSA, 0,1 % Tween 20 and 1X TBS), instead of 5 % non-fat milk. The same BSA blocking solution was used for antibodies dilutions, although, the temperature and the time of incubation were the same as described before. Results were analyzed with ImageJ® and Adobe Illustrator.

Primary antibodies used in this study are listed in **Table 8.2** (supplementary data) and correspond to the same used for IF. A mouse anti-β-actin antibody (Sigma-Aldrich #MA1-91399) was used as the WB loading control. As secondary antibodies a goat anti-mouse IgG labeled with Horseradish Peroxidase (HRP) (Thermo Fisher #31432) and a mouse anti-rabbit labeled with HRP (Thermo Fisher #31464) were used.

3.5 AGR2 Knock-Down Strategy

3.5.1 TRC2-Lentiviral Plasmid Vector TRC2-pLKO-puro Features

The vector used to knockdown AGR2 gene was the TRC2-Lentiviral Plasmid Vector TRC2-pLKO-puro (Mission shRNA Bacterial Glycerol stock Sigma-Aldrich #SHCLNG) (**Figure 3.2**). This shuttle vector contains a bacterial ampicillin resistant gene as well as a puromycin resistance gene for mammalian cells. Generation of the lentiviral particles containing this plasmid was performed at the Molecular Biology Platform at the Champalimaud Foundation (Lisbon, PT).

3.5.2 Plasmid Amplification

In brief, 18µL of the bacterial stock were added to 500 µL of LB medium without antibiotics. The culture was incubated for 30 minutes by shaking at 37 °C. Then, using a sterile loop, 25 µL of the incubated culture were spread into a freshly prepared plate containing LB agar and carbenicillin for selection of the ampicillin resistant bacteria. The use of carbenicillin, an ampicillin analog, was favored over ampicillin due to its increased stability in cultures. The plate was incubated overnight in a humidified atmosphere at 37°C. One single colony was isolated and added to LB liquid medium. The plasmid DNA was extracted using EndoFree Plasmid Maxi Kit (Qiagen #12362) by following the manufacter's protocol[59]. DNA integrity was verified by digestion with restriction enzymes HindIII, SacI and BamHI enzymes. The selection of the restriction enzymes was based on bioinformatics software (Snapgene) that, through plasmid sequence, detects which and where restriction enzymes hydrolyze the plasmid (**Figure 3.2 B**) and which one hydrolyze

shRNA sequence (**Figure 3.2 A**) and show the expected pattern of the restriction enzyme digestion gel (**Figure 3.2 C**). The experimental agarose gel corresponded with that of the one from the software (**Figure 3.2 D**), meaning that the plasmid was validated and virus production could be initiated.

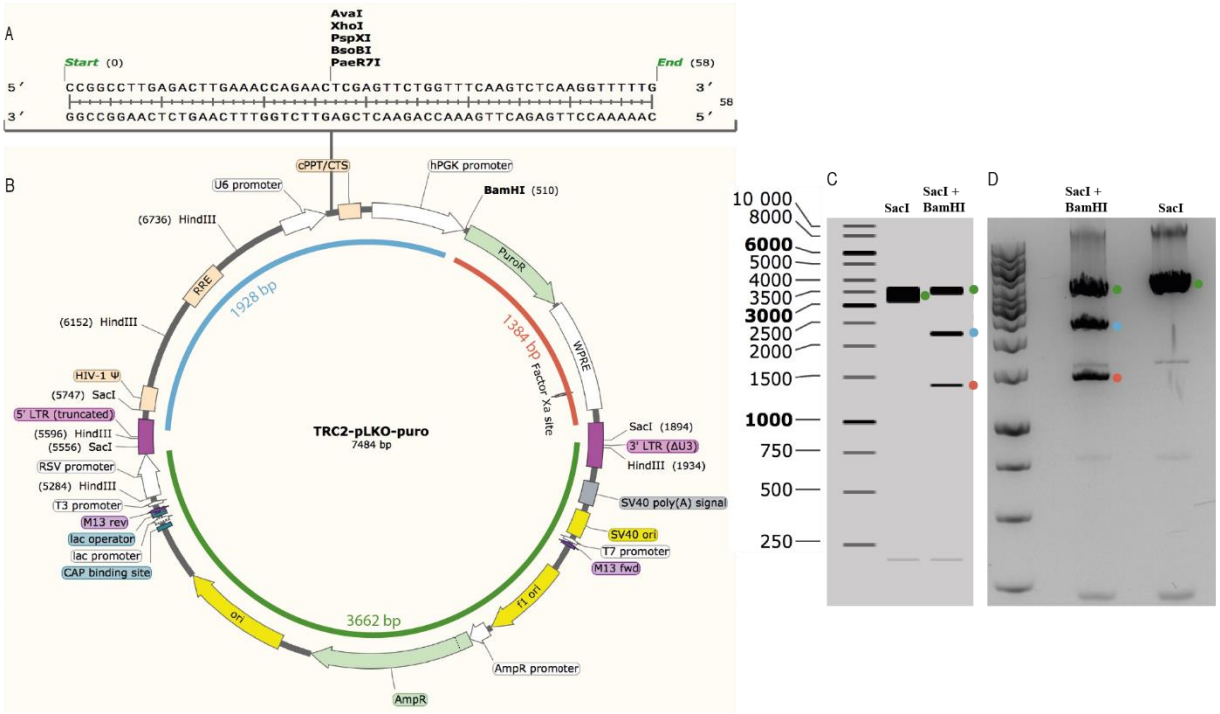

Figure 3.2 TRC2-Lentiviral Plasmid Vector TRC2-pLKO-puro. A: shRNA sequence that is encoded between U6 promoter and cPPT of the plasmid and has a size of 58 base pairs (bp). AvaI, XhoI, PspXI, BsoBI and PaeR7I are the restriction enzymes that hydrolyze the shRNA sequence and, for that reason are not good enzymes to be used in performing the plasmid validation. **B:** TRC2-pLKO-puro is the plasmid that contains the shRNA sequence to knock down *AGR2* gene and it has a size of 7484 bp. This plasmid includes U6 (U6 promoter), cPPT (Central polypurine tract), hPGK promoter (Human phosphoglycerate kinase eukaryotic promoter), puroR (Puromycin resistance gene for mammalian selection), WPRE (Woodchuck Hepatitis Post-Transcriptional Regulatory Element), 3'LTR (3' self-inactivating long terminal repeat), SV40 poly (A) signal, SV40 ori, T7 promoter, M13 fwc, f1 ori (f1 orgin of replication), ampR promoter (Ampilicin resistance gene for bacterial selection), ori (origin of replication), CAP (Catabolite activator protein) binding site, lac promoter, lac operator, M13 rev, T3 promoter, RSV promoter, 5' LTR (5' long terminal repeat), RRE (Rev response element). SacI and BamHI are the restriction enzymes used to validate the plasmid, SacI enzyme cuts the plasmid in two similar fragments, approximately 3662 pb (green line), SacI plus BamHI enzymes hydrolyze the plasmid and form three different fragment: 3662 bp (green line), 1928 bp (blue line) and 1384 bp (red line). **C:** Expected agarose gel (1%) of the restriction enzymes digestion with the chosen enzymes given by the software. The fragment marked with a green circle corresponds to the fragment formed by SacI and SacI + BamHI hydrolyze (green line in B) and has a size of 3662 bp. The fragment marked with a blue circle corresponds to the fragment formed by SacI + BamHI hydrolize (blue line in B) and has a size of 1928 bp. The fragment marked with a red circle corresponds to the fragment formed by SacI + BamHI hydrolyze (red line in B) and has a size of 1384 bp. **D:** Agarose gel (1 %) of the restriction enzyme digestion of the amplified plasmid. The fragment marked with a green circle corresponds to the fragment formed by SacI and SacI + BamHI hydrolise (green line in B) and has a size of 3662 bp. The fragment marked with a blue circle corresponds to the fragment formed by SacI + BamHI hydrolize (blue line in B) and has a size of 1928 bp. The fragment marked with a red circle corresponds to the fragment formed by SacI + BamHI hydrolise (red line in B) and has a size of 1384 bp.

3.5.3 Lentivirus Production

The 293T cells were maintained with DMEM medium supplemented with 10 % FBS at 37°C in humidified atmosphere of 5 % CO_2 in a 15 cm^2 plate until reaching a confluency of approximately 90%. In the following day, the medium was replaced with 15 mL of OptiMEM and 10 % of FBS. Lipofectamine was prepared (2,5 mL of OptiMEM and 99,36 µL of Lipofectamine 2000 (Thermo Fisher #11668027) and

then, it was incubated at RT for 5 minutes. DNA mixes were prepared according to the manufacter's instructions, combined with lipofectamine and incubated at RT for 20 minutes. This mix was added to cells drop wise (5,1 mL per plate) and it was incubated at 37 °C. In the following day, the medium was removed, replaced with 15 mL of fresh DMEM medium with 10 % FBS and was incubated at 37°C, again. Viral supernatant was collected and spin-down at 3000 x g for 3 minutes, after one day. The supernatant was filtered with 0.45 µm filter cup. To concentrate the virus, LentiX Concentrator (Clontech #631231) was used and combined 3:1 of supernatant and lentiX, respectively. The mix was incubated at 4°C overnight. In the following day, virus concentration procedures were repeated and mixed with the first one, both having been centrifuged at 1500 x g for 45 minutes, followed by supernatant removal. Pellets were ressuspend in 1/100 in 1X PBS and mixed. The aliquots were stored at -80 °C.

3.5.4 Transfection of Cells

A group of 100 000 cells of RT112_L_C and BFTC_L_C lines were grown and maintained on 6-well plates with medium as described in the section '3.1'. In the following day, the cells were infected. To transfect the cells, 10 µL of polybrene (10 mg/mL) (Thermo Fisher #TR-1003-G) were added to 10 mL of medium into a 15 mL sterile falcon tube. Then, 75 µL of the medium was added to 50 µL of the viral suspension into an eppendorf tube. In each well, 2 mL of medium with polybrene and 25 µL of viral mix were added. Plates were centrifuged at 600 rpm for 1 hour at RT. Afterwards, plates were incubated at 37 °C in a humidified atmosphere of 5% CO_2 overnight and, in the next day, the procedure was repeated. After two infections, 2 mL of fresh medium plus 2 µg/mL of puromycin (Gibco #A11138-02) were added to the cells in order to select those transfected. When cells were 90% confluent, the pellets were prepared to extract RNA and protein. During this process, fresh medium with puromycin was changed every two days. RNA was extracted and used to perform qRT-PCR as described in section '3.2'. The protein was extracted and used to produce WB as described in section '3.4'. Cells were plated in coverslips and IF performed as described in section '3.3'.

3.6 Invasion Assays

Invasion assay was performed using CytoSelect™ 24-well Cell Invasion Assay Kit (Cell Biolabs #CBA-110). The principle of invasion assay is to distinguish invasive cells from non-invasive cells. Invasive cells are able to degrade the matrix of proteins in the layer, and ultimately pass through the pores of the polycarbonate membrane, where they can be stained and quantified. On the day prior to the experiment, the medium of the cells was replaced with fresh medium without FBS (starvation). After rehydration of the basement membrane layer of the cell culture inserts, 180 000 cells of each cell line were transferred to a chamber and cells were growing with medium without FBS, however, outside of the chamber (inside of the well in a 24-well plate) there was medium supplemented with 10% of FBS.

To accomplish the specific number of cells for each experiment we counted cells with a hematocymeter. After trypsinization, the cells were centrifuged at 1200 rpm for 3 minutes at 4 °C. The supernatant was removed and pellet was re-suspended with 4 mL of cold 1X PBS. All these procedures were performed at 4ºC. To obtain cell count of the suspension, 10µL of solution were mixed with 10 µL of Trypan Blue 0,2% (Gibco), with a 1:1 dilution. After mixing, 10µL of the mix was pipetted into the hemacytometer chamber and observed with an inverted microscope under a 10X objective with phase

contrast to distinguish viable cells (shiniest cells are the viable cells, blue-stained cells are non-viable). To calculate the number of viable cells (nVC) per mL of solution, the following formula (**Equation 3.2**) was applied:

Equation 3.2:

$$nVC \times 10^4 \times L = \frac{cells}{mL}$$

L=dilution

The plate was incubated for 48 hours at 37 °C in 5% CO_2 atmosphere. After 48 hours, the medium without FBS was removed, the inserts were stained with 400 µL of Cell Stain Solution and incubated for 10 minutes at RT. After the inserts were washed, 200 µL of Extraction Solution were added to each well and the plate was incubated for 10 minutes at RT on an orbital shaker. Each sample was transferred to a 96-well plate and measured at 562 nm in a plate reader (BioTek #ELx800UV). For this procedure, manufacturer's instructions were followed.

3.7 Cell Proliferation assay

Cell proliferation assay allowed studying the proliferative capacities of the cells and it was performed using CellTiter® 96 Aqueous Non-Radioactive Cell Proliferation Assay Kit (Promega #G5421). In order to measure the relative number of viable cells MTS [3-(4,5-dimethylthiazol-2-yl)-5-(3-carboxymethoxyphenyl)-2-(4-sulfophenyl)-2H-tetrazolium] assays were done. The same number of cells (10 000 cells per well) were grown and maintained on 96-well plates. At 12, 24, 36, 48 and 72 hours, 20 µL of a 1:20 PMS/MTS solution were added to each well. The plate was incubated for 2 hours at 37 °C in a humidified and 5 % CO_2 atmosphere. Absorbance was measured using a plate reader (BioTek #ELx800UV) at a wavelength of 490 nm. In every experiment, the absorbance of the MTS/PMS + medium solution without cells was always measured as a control. For this procedure, the manufacture's introductions were followed.

3.8 Cell Cycle Analyses

Cell cycle analysis is a method to distinguish cells in different phases of the cell cycle through flow cytometry. One million cells were maintained as described in '3.1'. The cells were centrifuged at 1500 rpm for 5 minutes, ressuspended with 500 µL of 1X PBS and with 500 µL of cold 2 % PFA solution. Cells with PFA were incubated at 4°C for 1 hour. The suspension was centrifuged at 1500 rpm for 5 minutes and the pellet was ressuspended in 1X PBS. To fix the cells, 1 mL of cold 70 % ethanol was added drop wise doing vortex at the same time, to avoid cell agglomeration caused by ethanol. The cells were maintained in 70 % ethanol overnight at 4 °C. On the following day, cells were centrifuged at 1500 rpm for 5 minutes and washed with PBS for 10 minutes on ice to rehydrate. Centrifuge was repeated for 5 minutes at 1500 rpm and cells were ressuspended with 250 µL of PBS. 5 µL of 10 mg/mL of RNase A (Thermo Fisher #EN0531) were added to the suspension and incubated for 30-60 minutes at 37°C. The final procedure was to add 10 µL of 1 mg/mL of propidium iodide (PI, Sigma #P4170-10MG) solution and solution was kept in the dark

at 4°C for at least 10 minutes or until analysis. Data was acquired on LSR Fortessa X20 cytometer with a blue laser (488 nm for GFP detection) and yellow-green laser (561 nm for PI detection). For each sample, at least 50 000 events were collected and data analysis was performed using ModFit LT™ version 4 with Watson Model for cell analysis after aggregate exclusion. Images were extracted from FlowJo® version 10.3.

The cell cycle analysis was performed with the help of the Flow Cytometry Platform of the Champalimaud Foundation (Lisbon, PT).

3.9 *In Vivo* Bladder Orthotopic Model

3.9.1 Inoculation of Bladder Cancer Cells

To perform studies *in vivo*, $1x10^6$ bladder tumor cells were inoculated in each Non-Obese Diabetic/Severe Combined Immuno Deficient (NOD/SCID) 5-7 weeks-old female mice. 5 mice for each cell line were used.

Before given the injections, mice were first anesthetized in an induction chamber with 2-3% isoflurane and 0,5 mb O_2, until not showing any reflexes. Mice were placed in supine position (on their back) on the face mask with 2-3% isoflurane on a warming path. 100 µL of cell solution containing the one million cells at RT were inoculated on the bladder of the female through the urethra, as previously described in the literature[60], the catheter being kept inside the mice's bladder for 30 minutes. The tail of the animals was marked with a permanent ink to distinguish them. The animals were checked and weighted every two days, to assess performance status. 4 weeks after the inoculation, *in vivo* imaging with the IVIS Spectrum system (Perkin-Elmer) was performed at the IMM (Lisbon, PT) to determine tumor progression as previously described.

3.9.2 In Vivo Bioluminescent Imaging (BLI)

Luciferin is a common bioluminescent reporter used for *in vivo* imaging of the expression of luciferase. Luciferase enzyme utilizes ATP and Mg^{2+} as co-factors to emit a characteristic yellow-green emission in the presence of oxygen, which shifts to red light *in vivo* at 37 °C. Experimental cell lines were originally transfected with the firefly luciferase gene (**Figure 3.1**) and intra-peritoneal injection of D-luciferin (150 mg/kg of body weight, PromoKine #PK-CA707-10101-2), permitted the evaluation of tumor progression *in vivo* through BLI. For this procedure, the manufacturer's instructions were followed.

3.9.3 Histopathological Assessment

After imaging, mice were sacrificed and all organs were fixed in 4% buffered formalin and processed. The sections were stained with Hematoxylin & Eosin (H&E) in the Histology and Comparative Pathology Laboratory of the IMM (Lisbon, PT). The slides with the sections were scanned in Pathology Platform of Champalimaud Foundation and images analyzed by Adobe Illustrator.

3.10 Statistical Analysis

The statistical analysis was performed using SPSS® software version 24 (SPSS, Chicago, USA). The normality of the samples in the study was tested with Kolmogorov-Smirnov test. The comparison of means of qRT-PCR, WB, IF, cell cycle, proliferation and invasion assays results were tested with student t test when there were two sets, and ANOVA when were three categories. Whenever samples did not follow normality, non-parametric tests were used, such as Kruskal-Wallis when there were three sets of samples. A p-value < 0.05 (double-sided) was considered statistically significant. Except invasion assay, all experiments were performed in triplicate and repeated at least twice. Data are presented as mean ± standard deviation (SD) from 3 independent experiments.

4 Results

Previously, work developed by our group showed that HG-NMIBC cell lines with loss of ΔNp63 display higher proliferation rate *in vitro* and *in vivo*, higher invasion capacity *in vitro* and higher metastatic potential in an *in vivo* mouse model compared to cells with ΔNp63 expression (unpublished data). To validate these results, the orthotopic *in vivo* mouse assay was repeated in Lisbon with the RT112 cell line. $1x10^6$ cells were injected in the bladder of each female NOD/SCID mice and imaging in the IVIS was performed after 4 weeks. Consistent to previous findings, a higher tumor formation in the bladder was observed, as well as higher frequency in formation of metastasis formation in the kidneys in mice inoculated with ΔNp63 knock-down cells when compared to parental lines ($\Delta Np63^+$) (**Figure 4.1 A**). Mice were sacrificed after imaging and their organs (bladder, heart, lungs, liver, kidney, spleen and thymus) were fixed in 4% buffered formalin and embedded in paraffin for histological evaluation (**Figure 4.1 B**).

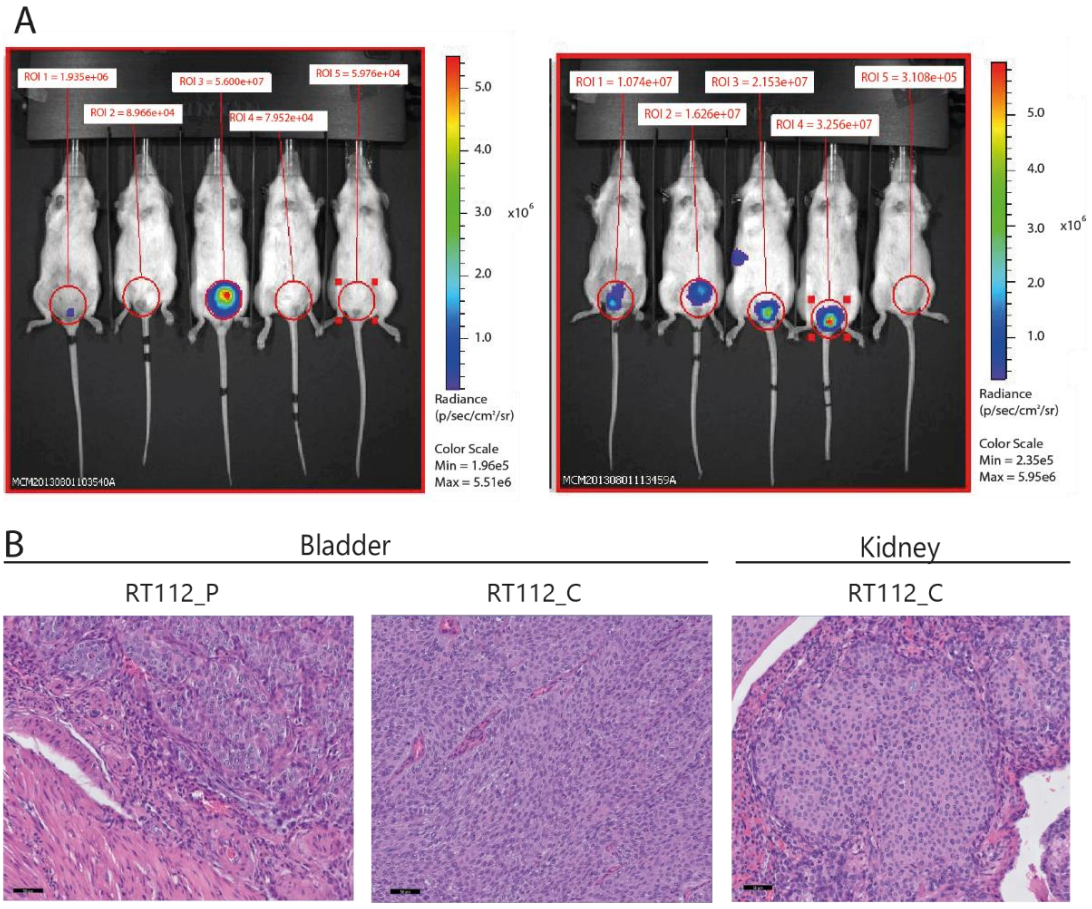

Figure 4.1 NMIBC cells with loss of ΔNp63 generate more tumors with a more aggressive phenotype. A: Mice inoculated with parental cells (left panel, $\Delta Np63^+$) developed less tumors in the bladder than mice inoculated with clone cells (right panel, $\Delta Np63^-$). (Images are from Mireia Castillo's work in Dr. Cordon-Cardo's Laboratory, Icahn School of Medicine at Mount Sinai, New York, USA). **B:** Histology analysis of the organs from NOD/SCID female mice four weeks after inoculation with RT112_L_P and RT112_L_C cells. Bladder tumor formation was higher in mice inoculated with RT112_L_C than with RT112_L_P, and kidney metastasis were only observed in mice inoculated with RT112_L_C. Scale bar: 50 µm. Organs were fixed in formalin, paraffin embedded and stained with H&E by the Histology and Comparative Pathology Laboratory of the IMM (Lisbon, PT).

Gene expression analyses previously performed by Dr.ª Mireia Castillo comparing parental lines and clones with ΔNp63 knock-down (BFTC and RT112) revealed that there were nine (*AGR2*, *CAPS*, *CHD2*, *GCHFR*, *HOXC6*, *HRK*, *LRRC26*, *SORBS2* and *S100A4*) and four (*EPDR1*, *PPARG*, *SCML1* and *SPOCK1*) commonly up-regulated and down-regulated genes, respectively, amongst the experimental cell lines. After literature review about their relevance in cancer, and search for primers and antibodies availability, four out of the nine up-regulated genes (*AGR2*, *HOXC6*, *HRK* and *S100A4*) and two out of the four down-regulated genes (*SCML1* and *SPOCK1*) were chosen for further studies in this work. To validate gene expression analyses, mRNA expression was analyzed through quantitative real-time PCR. The difference of expression between the knock-down ΔNp63 cells (clones: BFTC_L_C and RT112_L_C) and the wild type cells (parental: BFTC_L_P and RT112_L_P) was compared, for each gene with GAPDH as internal control, in triplicate (**Figure 4.2 A**). These results showed that according to the RNA microarrays results, *HRK* mRNA showed a tendency of up-regulation in both bladder cancer cell lines whereas *AGR2* mRNA showed statistically significant increased levels in BFTC_C and *S100A4* mRNAs had a tendency of up-regulation in BFTC_L_C cells (blue) and down-regulation in RT112_L_C cells (red). On the contrary, *HOXC6*, *SCML1* and *SPOCK1* mRNAs showed a tendency of down-regulation in the ΔNp63 knock-down cells.

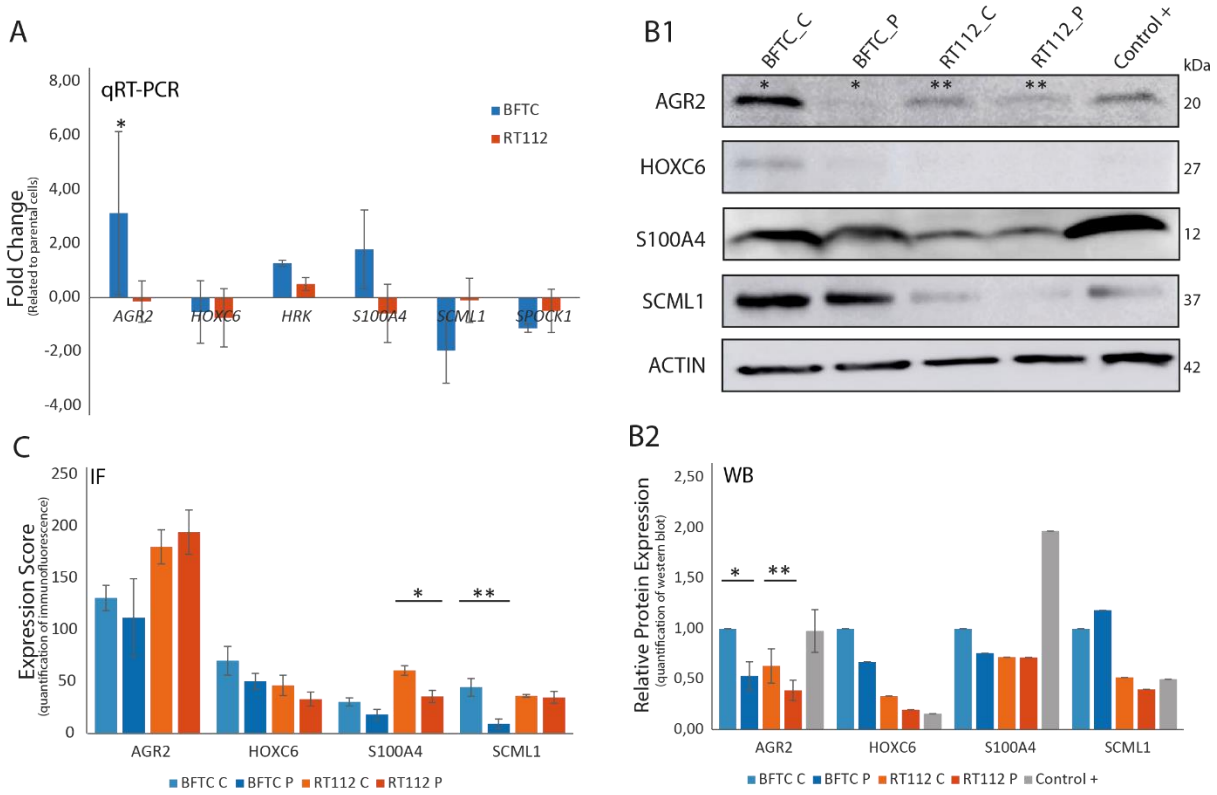

Figure 4.2 mRNA and protein expression in BFTC_L_P, BFTC_L_C, RT112_L_P and RT112_L_C and control cell lines. A: mRNA expression of *AGR2*, *HOXC6*, *S100A4*, *SCML1* and *SPOCK1* through qRT-PCR. Comparison between cells with ΔNp63^{+} (P) and ΔNp63^{-} (C). Data were normalized against *GAPDH* within the same sample. BFTC cells are represented in blue columns ± SD, n=3. RT112 cells are represented in red columns ± SD, n=3. Columns represent the mean from 3 separate experiments; each experiment was done in triplicates. *p-value < 0.05 by independent samples student t-test. **B-B1:** Western blot analysis of AGR2 (20 kDa), HOXC6 (27 kDa), S100A4 (12 kDa) and SCML1 (37 kDa) protein level in BFTC_L_P, BFTC_L_C, RT112_L_P, RT112_L_C and in positive control tumor cell line. β-actin expression was the internal control. **B2:** Quantification of WB assay. Experiments were done in triplicates. Dark and light blue columns represent BFTC_L_P and BFTC_L_C, respectively. Dark and light orange columns represent RT112_L_P and RT112_L_C, respectively. Grey column represents the positive control. *p-value (AGR2 in BFTC) = 0,053 **p-value (AGR2 in RT112) = 0,068 by independent samples t-test. **C:** Quantification of immunofluorescence images taken from Zeiss AxioImager M2 microscope with 20x amplification (Figure 8.1) *p-value < 0,01 **p-value < 0,05 by independent samples t-test.

In BFTC cell line, *AGR2*, *HRK* and *S100A4* mRNAs showed tendency of up-regulation in clones comparatively to parental cells and *SCML1* and *SPOCK1* mRNAs showed propensity of down-regulation in the same situation, similar to gene expression analysis. *HOXC6* mRNA had tendency of down-regulation in clones comparatively to parental cells in both NMIBC cell line which contradicts the results of gene expression analysis. In RT112 cell line, all of the tested mRNA (*AGR2*, *HOXC6*, *S100A4*, *SCML1* and *SPOCK1*) showed tendency of down-regulation in clones cells, with only *HRK* mRNA showing propensity of up-regulation in clone cells. *AGR2* mRNA overexpression in BFTC cell line was statistically significance. These results did not completely validate gene expression analysis and, for that reason, IF and WB assay were performed.

The study of protein expression was essential to validate the previous results and with this in mind, WB and IF assays were performed for the same genes (**Figure 4.2 B-C** and **Figure 8.1**). Optimization of the antibodies was performed using positive and negative controls before WB assays in our experimental cell lines, described in **Table 8.2**. WB results suggest that the AGR2 and HOXC6 protein expression are significantly higher in clones than in parental cells, in both of bladder cancer cell lines (**Figure 4.2 B**). The S100A4 protein level is higher in clones than in parental cells in BFTC, but it could not be confirmed in RT112 cells (**Figure 4.2 B**). SCML1 protein expression is higher in parental than in clones cells in BFTC cell line and the opposite occurs in RT112 cell lines (**Figure 4.2 B**). The SPOCK1 protein was excluded from the immunofluorescence assay and western blot assays, given the lack of good antibodies for this protein. The HRK was excluded to the western blot analysis because the anti-HRK antibody was not detecting any band of the pretended size. Protein expression and their subcellular location were studied through immunofluorescence staining (**Figure 4.2 C** and **Figure 8.1**). All the antibodies were optimized before in positive and negative controls, and the final dilutions used are described in **Table 8.2**. AGR2 protein is expressed in endoplasmic reticulum, HOXC6 and S100A4 are expressed in cell cytoplasm (**Figure 8.1 A-C**). SCML1 is expressed in the nucleus (**Figure 8.1 D**). AGR2 WB analyses were performed in triplicates, whereas all other tests were performed only once, with these results we can only observe a tendency of expression, and more experiments need to be done to test their statistical relevance.

Table 4.1 Summary of gene expression analysis, qRT-PCR, WB and IF results. The positive symbol (blue) correspond to results where the mRNA or protein is more expressed in clones than in parental cells. The negative symbol (orange) correspond to results where the mRNA or protein is less expressed in clones than in parental cells. Green circles mean that the result is not observable. Grey boxes indicated that the analysis was not performed. *AGR2*, *HOXC6*, *HRK* and *S100A4* has higher gene expression in clones than in parental cells, whereas the opposite happens with *SCML1* and *SPOCK1* genes. Through qRT-PCR assay, *AGR2* mRNA is higher expressed in clones in BFTC but is lower expressed in clones in RT112, as well as *S100A4*. *HRK* is higher expressed in clones than in parental in both bladder cancer cell lines. *HOXC6* mRNA is lower in clones than in parental cells in both cancer cell lines. *SCML1* and *SPOCK1* mRNA are lower in clones than in parental cells. WB results suggest that AGR2 protein is more expressed in clones than in parental cells, as well as HOXC6 and S100A4 genes. SCML1 protein is lower expressed in clones than in parental, in BFTC cell line and the opposite in RT112 cell line. IF results suggest that AGR2 is more expressed in BFTC clones than in parental and lower in RT112 clones than in parental, whereas HOXC6 and S100A4 are more expressed in clones than in parental cells, in both of bladder cancer cell lines.

Technique	Gene expression analysis		qRT-PCR		WB		IF	
Cell line	BFTC_L	RT112_L	BFTC_L	RT112_L	BFTC_L	RT112_L	BFTC_L	RT112_L
AGR2	⊕	⊕	⊕	⊖	⊕	⊕	⊕	⊖
HOXC6	⊕	⊕	⊖	⊖	⊕	⊕	⊕	⊕
S100A4	⊕	⊕	⊕	⊖	⊕	●	⊕	⊕
HRK	⊕	⊕	⊕	⊕				
SCML1	⊖	⊖	⊖	⊖	⊖	⊕	⊕	●
SPOCK1	⊖	⊖	⊖	⊖				

Through IF results, we observe a tendency of AGR2 protein expression showing higher intensity in clones than in parental cells, in BFTC cell line and the opposite in RT112 cell line (**Figure 4.2 C** and **Figure 8.1 A**). HOXC6 protein expression showed a tendency of higher expressed in clones than in parental, in both bladder cancer cell lines (**Figure 4.2 C** and **Figure 8.1 B)** as well as S100A4 protein expression (**Figure 4.2 C** and **Figure 8.1 C**). SCML1 protein expression is lower in clones than in parental cells in BFTC cell line and the contrary tendency is observed in RT112 cell line (**Figure 4.2 C** and **Figure 8.1 D**). The up-regulation of S100A4, in RT112_C, and SCML1, in BFTC_C was statistically significant.

After reviewing all the obtained results from the mRNA and the protein expression analyses of AGR2, HOXC6, HRK, S100A4, SCML1 and SPOCK1, summarized in **Table 4.1**, we centered our future experiments to analyze *AGR2* function in bladder cancer tumor progression. To test our hypothesis, *AGR2* gene was knock-down in BFTC_L_C cells, which had previously been ΔNp63 knocked down. After shRNA stable knock-down of *AGR2*, total RNA and protein were extracted and levels of *AGR2* mRNA and protein were tested by qRT-PCR, WB and IF assays (**Figure 4.3**).

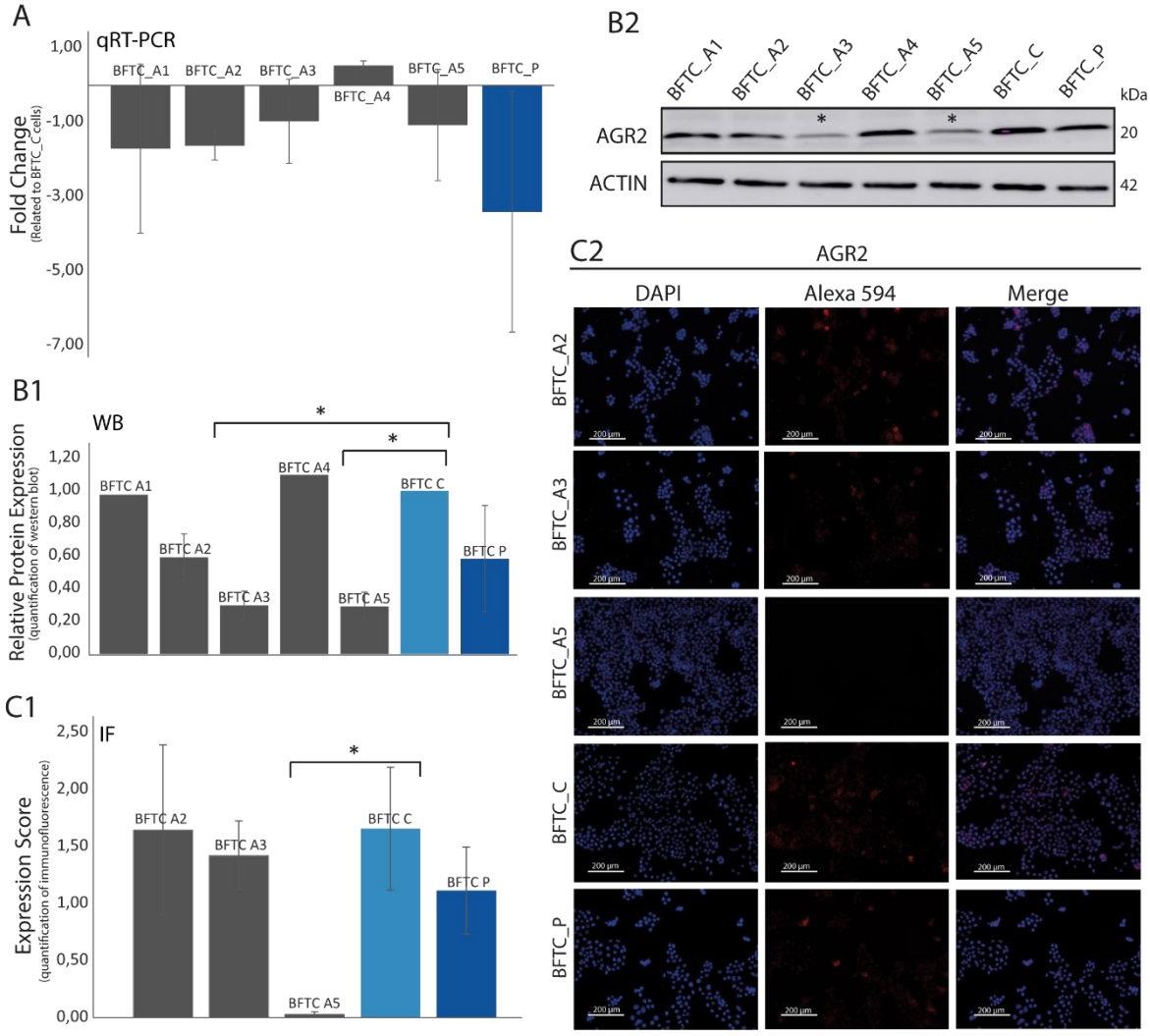

Figure 4.3 mRNA and Protein expression in *AGR2* knock down BFTC cell lines (clones A1, A2, A3, A4 and A5).

Figure 4.3 mRNA and Protein expression in *AGR2* knock down BFTC cell lines (A1, A2, A3, A4 and A5). A: mRNA expression level of *AGR2* gene through qRT-PCR. The expression of *AGR2* gene was compared between the cells with ΔNp63^{+} phenotype (BFTC_P), ΔNp63^{-} phenotype (BFTC_C) and ΔNp63^{-} AGR2^{-} phenotype (BFTC_A). All data were normalized against levels of *GAPDH* mRNA expression within the same sample. Columns represent the mean from three separate experiment and each experiment was done in triplicates. The results do not have statistical significance testes with independent t-test against BFTC_C. **B-B1:** Quantification of western blot analysis of AGR2 (20 kDa) protein level in BFTC_A1, BFTC_A2, BFTC_A3, BFTC_A4, BFTC_45, BFTC_C and BFTC_P. BFTC_A2, BFTC_A3, BFTC_A5, BFTC_C and BFTC_P experiments were done in triplicates. *p-value < 0,05 by independent samples t-test against BFTC_C. **B2:** Representative western blot membrane of AGR2 protein. β-actin protein expression was the internal control. **C-C1:** Quantification of immunofluorescence assay using anti-AGR2 antibody in BFTC_A2, BFTC_A3, BFTC_A5, BFTC_C and BFTC_P. *p-value < 0,05 by independent samples t-test against BFTC_C. **C2:** Representative immunofluorescence images taken from Zeiss AxioImager M2 microscope with 20x amplification. The grey column represents the cells knocked-down for ΔNp63 isoform and *AGR2* gene ± SD, n=3, light blue column represents the BFTC_C cells ± SD, n=3 and dark blue column represents the BFTC_P ± SD, n=3.

The qRT-PCR results showed that BFTC_A1, BFTC_A2, BFTC_A3 and BFTC_A5 present lower levels of *AGR2* compared with BFTC_C, which after knockdown for ΔNp63 showed increased levels of this gene in comparison with BFTC_P cells. However, BFTC_A3 and BFTC_A5 were the cells with higher knockdown efficiency and consequently the ones with the lowest level of *AGR2* mRNA expression. Notably, BFTC_A4 showed no decrease of *AGR2* expression (**Figure 4.3 A**). The WB results validated the qRT-PCR results. Except BFTC_A4, all of the cells knocked down for AGR2 showed lower levels of this protein and those with the lowest level were BFTC_A3 and BFTC_A5 (**Figure 4.3 B1-B2**). The IF results were performed only in BFTC_A2, BFTC_A3 and BFTC_A5 because they corresponded to the cell lines with the lowest level of AGR2 protein. BFTC_A5 was the cell line with lowest level expression of AGR2 protein by IF (**Figure 4.3 C1-C2**). In conclusion, qRT-PCR, WB and IF results identified BFTC_A5 as the clone with lowest level of AGR2 and for this reason that cell line was used to test the main hypothesis of this project: that without AGR2 protein, bladder NMIBC tumor cells would be less invasive, less proliferative and less aggressive. To study that, different *in vitro* experiments, such as cell cycle, proliferation and invasion assays were performed.

The cell cycle was analyzed by comparing the ratio between the number of cells in G2 and G1 phases. The results showed that BFTC_C (ΔNp63^{-} *AGR2*$^{+}$) had the highest G2/G1 ratio, followed by BFTC_A5 (ΔNp63^{-} *AGR2*$^{-}$) and the lowest ratio in BFTC_P (ΔNp63^{+} *AGR2*$^{+}$). This means that after knocking down *AGR2* in previously ΔNp63 knocked down cells, these cells have lower cell division, although not reaching the low levels of BFTC_P (ΔNp63^{+} *AGR2*$^{+}$) (**Figure 4.4 A1-A2**). The proliferation assay analyzes the activity of the cell and these results showed that BFTC_C (ΔNp63^{-} *AGR2*$^{+}$) cells displayed higher proliferation rate than BFTC_P (ΔNp63^{+} *AGR2*$^{+}$) and BFTC_A5 (ΔNp63^{-} *AGR2*$^{-}$) cells *in vitro* (**Figure 4.4 B**). Finally, BFTC_C (ΔNp63^{-} *AGR2*$^{+}$) cells showed higher invasion capacity when compared with BFTC_P (ΔNp63^{+} *AGR2*$^{+}$) and BFTC_A5 (ΔNp63^{-} *AGR2*$^{-}$) cells *in vitro* (**Figure 4.4 C**). Overall, BFTC_P (ΔNp63^{+} *AGR2*$^{+}$) showed lower cell division, lower cell proliferation and lower cell invasion *in vitro*, whereas BFTC_C (ΔNp63^{-} *AGR2*$^{+}$) cells showed the highest cell division, the highest cell proliferation and the highest cell invasion *in vitro*. Moreover and in concordance with our hypothesis, BFTC_A5 (ΔNp63^{-} *AGR2*$^{-}$) behaved in a similar way than BFTC_P (ΔNp63^{+} *AGR2*$^{+}$), going back to a less aggressive phenotype, results that suggest that *AGR2* expression is important in tumor aggressiveness/progression.

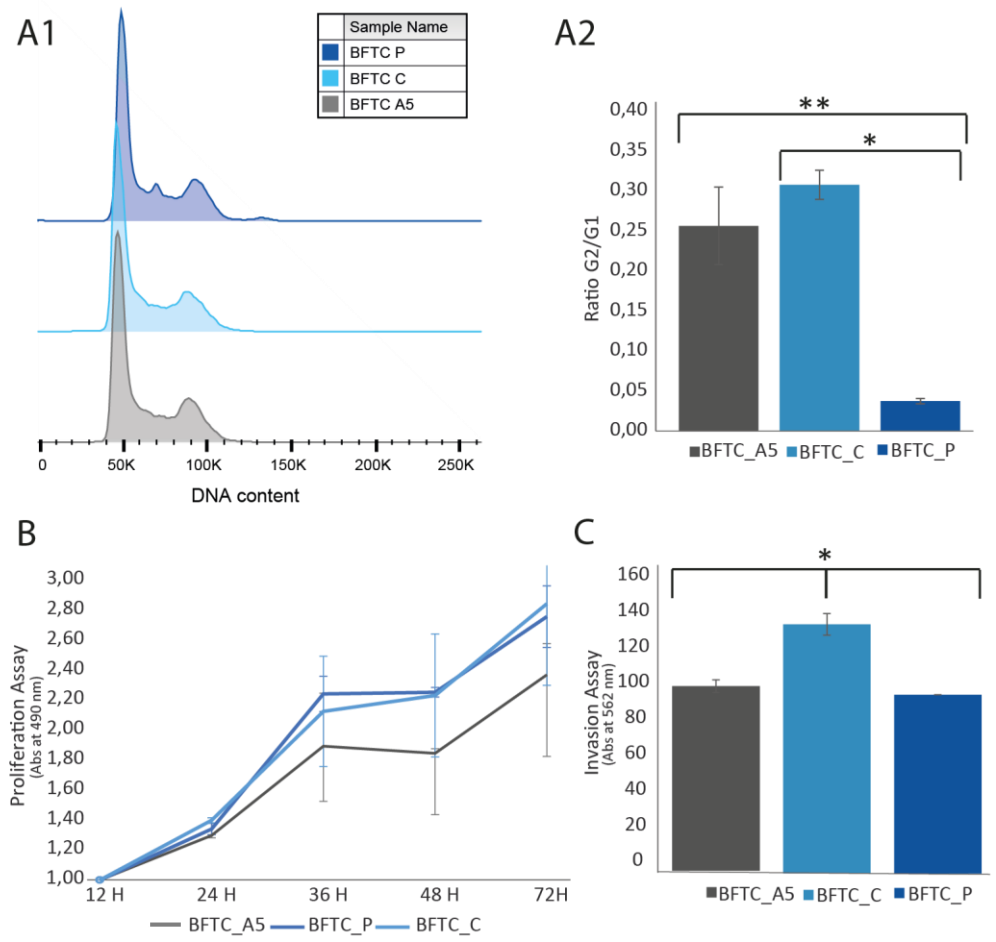

Figure 4.4 Functional studies of BFTC_A5, BFTC_C and BFTC_P cell lines. A-A1: Representation of cell cycle results obtained by Flow Cytometry. The higher pick in 50K correspond to the G1 phase, while the pick in the 100K correspond to G2 phase and between G1 and G2 phase is the S phase of the cell cycle. **A2:** Bar diagram of G2/G1 ratio of the cell cycle assay, n=2, in triplicates. Grey column represents the cells knocked-down for ΔNp63 isoform and *AGR2* gene (BFTC_A5) ± SD, light blue column represents the BFTC_C cells ($\Delta Np63^-$) ± SD and dark blue column represent the BFTC_P ($\Delta Np63^+$) ± SD. *p-value = 0,002 **p-value = 0,004 by independent samples ANOVA test. **B:** Proliferation assay of BFTC_A5, BFTC_C and BFTC_P. Absorbance at 490 nm of cells and MTS were measure in 5 points for 72 hours. Grey line represents the cells knocked-down for ΔNp63 isoform and *AGR2* gene (BFTC_A5) ± SD, n=3, light blue line represent the BFTC_C ($\Delta Np63^-$) cells ± SD, n=3 and dark blue line represent the BFTC_P ($\Delta Np63^+$) ± SD, n=3, in quadruplicates. No significant results were observed by independent samples ANOVA test. **C:** Bar diagram of invasion assay of BFTC_A5, BFTC_C and BFTC_P cell line measure at 562 nm, n=1, in quadruplicates. Grey column represents the cells knocked-down for ΔNp63 isoform and *AGR2* gene (BFTC_A5) ± SD, light blue column represent the BFTC_C cells ($\Delta Np63^-$) ± SD and dark blue column represent the BFTC_P ($\Delta Np63^+$) ± SD. *p-value = 0,013 by independent samples Kruskal Wallis test.

5 Discussion

The main goal of this project was to discover the genetic alterations associated with this ΔNp63 loss, *TP63* isoform, which confer the aggressive phenotype to tumor cells. In the previous results of our group, it was observed that tumors with loss of ΔNp63 (BFTC_L_C and RT112_L_C) had higher proliferation rate both *in vitro* and *in vivo* as well as increased colony formation activity (unpublished data). Furthermore, these cells displayed superior invasion capacity *in vitro*, which correlated with higher local tumor initiation and metastatic potential in an orthotopic *in vivo* mouse model. The role of ΔNp63 in cancer is not well known. Karni-Schmidt *et al.* described that ΔNp63 can be a protective factor and act like a tumor suppressor in NMIBC however, this p63 isoform seems to have the opposite function in MIBC, where it has an oncogenic role[61]. This antagonist role could be a consequence of the expression of the different ΔNp63 isoforms (α, β and γ). These isoforms are not well known because there are no specific antibodies for each of them and because of that we are only studying the role of total ΔNp63 and assuming that the isoforms have the same role. In this work, we only studied HG NMIBC and total ΔNp63.

Gene expression analyses revealed that there were nine (*AGR2, CAPS, CHD2, GCHFR, HOXC6, HRK, LRRC26, SORBS2* and *S100A4*) and four (*EPDR1, PPARG, SCML1* and *SPOCK1*) commonly up-regulated and down-regulated genes in clones than in parental, respectively, amongst the experimental cell lines. To access the previous known involvement of all these genes in cancer biology, an extensive literature review was performed. After this research has been done, *CAPS, CHD2, GCHFR, LRRC26, SORBS2, PPARG* and *EPDR1* genes were excluded from this work because of the inability to construct specific primers, or due to the absence of good antibodies available or they did not have any evidence in tumor development. On the other hand, *AGR2, HOXC6, HRK, S100A4, SCML1* and *SPOCK* genes seemed interesting in the field of cancer.

To validate gene expression analyses, mRNA expression of the chosen genes was analyzed through quantitative real-time PCR. The results revealed that *AGR2* is higher expressed in clones ($\Delta Np63^-$) than in parental cells ($\Delta Np63^+$), only in BFTC cell line, although, in RT112 cell line seems that *AGR2* is more expressed in parental cells ($\Delta Np63^+$), however the difference is small. This result suggests that, in BFTC cell line, *AGR2* is up-regulated when ΔNp63 is not expressed. The mRNA of *HOXC6* is down-regulated in clones ($\Delta Np63^-$) when compared with the parental cells ($\Delta Np63^+$), in both BFTC and RT112 cell lines. The qRT-PCR result contradicts the gene expression analysis that had identified *HOXC6* has an up-regulated gene in the same genetic background. The mRNA expression of *HRK* is higher in clones ($\Delta Np63^-$) than in parental cells ($\Delta Np63^+$), in both of the NMIBC cell lines. The mRNA of *S100A4* is up-regulated in the clone cells ($\Delta Np63^-$) when compared to the parental cells ($\Delta Np63^+$) in BFTC cell line but not in the RT112 cell line. *SCML1* and *SPOCK1* mRNA levels are down-regulated in clone cells ($\Delta Np63^-$). For the *AGR2, HOXC6* and *S100A4* mRNA, RT112 cell line showed to express lower levels of all of the mRNA when ΔNp63 is not expressed (clones), which contradicts the gene expression results. *SCML1* and *SPOCK1* mRNAs exhibited lower levels and *HRK* mRNA exhibited higher level in clones ($\Delta Np63^-$) than in parental ($\Delta Np63^+$), in both NMIBC cell lines, which correlates with gene expression analysis. BFTC cell line exhibited higher levels of *AGR2, HRK* and *S100A4* mRNA and lower levels of *HOXC6, SCML1* and *SPOCK1* mRNA, when ΔNp63 is not expressed. All mRNAs studied by qRT-PCR, except AGR2 in BFTC cell line, did not show any statistical significance so the qRT-PCR results showed only a tendency of the mRNA expression.

The qRT-PCR results were not enough to validate the gene expression analysis because in some cases the results were not consistent with the gene expression microarray. Morey *et al.* reported that microarrays and qPCR data often result in disagreement and refer some factors that can contribute to that, such as the biological variability, the quality of RNA, the fold change and other factors. The biological variability cannot be controlled but it has to be considered. The quality of RNA is essential to obtain results, it can be affected by carry-over of contaminating factors and salts, alcohols, phenol, and other contaminating factors, which can affect reverse transcriptase used in qRT-PCR[62]. Moreover, gene expression is analyzed by informatics software and sometimes the results from this technique are not reproducible *in vitro*.

Differences of results were not only observed between different techniques, but also between different NMIBC cell lines by the same technique. BFTC and RT112 cell lines are human high risk non-muscle invasive bladder cancer cells, tumors with elevate risk for progression to MIBC, developed several decades ago from women. Notably, they both show a mutation in *TP53* gene. *TP53* encodes the TP53 protein that is located in the nucleus of the cells and attached to the DNA, this protein has a role in damaged DNA repair and apoptosis, leading to preventing the tumor formation. Mutations in the *TP53* tumor suppressor are the most frequent genetic alterations in cancer, these mutations have been associated with tumor progression and poor patient survival[63–65]. In bladder tumor, TP53 protein has also been reported as tumor progression factor[66–68]. The aim of this project was to study the NMIBC progression and to test whether an isoform of *TP63*, ΔNp63, was associated with this progression. For that reason, BFTC and RT112 were the chosen cell lines, both have *TP53* mutation which is a factor of more aggressiveness phenotype and with this NMIBC cell lines was easier to verify if *TP63* isoform was involved in tumor progression or not. However, the BFTC and RT112 cell lines showed different results when we performed qRT-PCR of the genes of interest was performed, which certainly could be consequence of a different genetic background. A study to compare the common mutations between BFTC and RT112 cell lines and a panel of the 409 genes most frequently altered in cancer was performed[69] (**Figure 8.2** (supplementary data)). BFTC cell line presented 447 mutations but only 18 were common genes in the Ion Torrent panel, which are *BAI3, BCL9, PKHD1, NRAS, BLM, TNK2, CDH11, PTCH1, ARID2, CDH20, TRRAP, SRC, IFGA9, FOXP1, SAMD9, DCC, CSFR1* and *SOX2*. We found that some of these genes were found to have a role in bladder tumor, such as *ARID2* gene, which is considered a tumor suppressor that has function as chromatin remodeler, modulation of transcription and suppress cancer formation[70]. Moreover, *SOX2* gene has been reported in bladder cancer specimens correlating with the presence of CIS and also the knockdown of *SOX2* gene in bladder cancer cells has been described to attenuate tumor growth[71,72]. The RT112 cell line presented 298 mutations but only 10 were common with the genes of the Ion Torrent panel, which are *KDM6A, EPHA7, NF1, MYC, PRDM1, FLCN, PIK3CA, HSP90AB1, CEBPA* and *HCAR1*. The *KDM6A* gene encodes a protein that has histone demethylase function and has been found mutated in MIBC[73]. The *MYC* is a regulator gene and plays a role in cell cycle progression, apoptosis and cellular transformation[74]. The *PIK3CA* encodes a subunit of PI3K protein that controls cell growth, tumorigenesis, cell invasion and drug response. The *PIK3CA* gene alterations have been associated with reduced recurrence in NMIBC[75]. Some of these gene mutations could be molecularly connected with ΔNp63 isoform and/or with the genes that were studied and could lead to this distinct performance of the bladder cancer cell lines. BFTC and RT112 cell lines showed 22 common mutated genes, which are *ESX1, NOS1, TENM4, APOB, ADAMTS2, AHNAK, TEMEM209, KIAA1551, KANSL1, NACA, MUC4, IBSP FAM83A, TRIM66, RYR2, ZNF853, MT-ND5, PRR12, KMT2C* and *PAPOLB*, but only one was in common with the 409 important genes in tumor biology panel, the *TP53* gene, as referred above.

To validate the qRT-PCR results, protein studies were done to study the protein levels, and WB and IF assays were performed. WB is a good approach to protein quantification while IF is a good technique to verify the subcellular localization of the protein and allowing also its quantification, thus, they are complementary methodologies for protein expression assessment. WB results showed that AGR2 protein is more expressed in clone cells (both BFTC_L_C and RT112_L_C, $\Delta Np63^-$) than in parental cells (BFTC_L_P and RT112_L_P, $\Delta Np63^+$), which strongly suggests that when ΔNp63 is lost, AGR2 expression increase. The same result was observed for HOXC6 protein. The S100A4 protein showed higher level in clones ($\Delta Np63^-$) than in parental ($\Delta Np63^+$) cells but only in BFTC cell line, in RT112 no difference was observed by WB. The SCML1 protein was higher in parental ($\Delta Np63^+$) than in clone cells ($\Delta Np63^-$), only in BFTC cell line, whereas in RT112 the parental ($\Delta Np63^+$) showed lower levels of this protein. These results suggest that when tumor cells have no expression of ΔNp63 isoform, AGR2, HOXC6 and S100A4 proteins are up-regulated and SCML1 protein is down-regulated. HRK protein was also measured by WB, however given that a band with a molecular weight different to what was supposed to be observed, it was concluded that the anti-HRK antibody was detecting another protein and, for that reason, this analyses through IF was discontinued. All proteins studied by WB, except AGR2, were performed only once so, with these results, we can only observe a tendency and more experiments need to be done to test their statistical relevance. IF results showed the subcellular location of the proteins and the difference in expression level between parental and clones cells. AGR2 protein is expressed in endoplasmic reticulum and appears to be more expressed in clones ($\Delta Np63^-$) than in parental ($\Delta Np63^+$), in BFTC cell line, and the opposite in RT112 cell line. HOXC6 and S100A4 proteins are expressed in the cell cytoplasm and this protein present higher level in clones ($\Delta Np63^-$) than in parental ($\Delta Np63^+$) cells, in both NMIBC cell lines. SCML1 is expressed in the nucleus and seems to be that is more expressed in clones ($\Delta Np63^-$) than in parental ($\Delta Np63^+$), only in BFTC cell line. The increased S100A4 protein level in RT112_C and the increased SCML1 protein level in BFTC_C were statistically significant, while the rest of the proteins levels were not.

Usually, when a mRNA is overexpressed so is the respective protein. However, sometimes mRNA expression is not consistent with protein expression. *AGR2*, for example, appears to have higher mRNA and protein expression in clones ($\Delta Np63^-$) comparatively to parental ($\Delta Np63^+$) cells, in BFTC cell line. On the contrary, in the RT112 cell line, *AGR2* displays lower mRNA expression and higher protein expression in clones ($\Delta Np63^-$) than in parental ($\Delta Np63^+$) cells. Down-regulation of mRNA concomitant with up-regulation of protein expression could be consequence of protein half-life increase due to stabilization of protein-protein interactions and due to the turnover of the protein could be disrupted, this means that the ratio between protein synthesis and protein degradation was disturbed. Another possible reason for this to occur could be that mRNA might be degraded by some unknown mechanism. Usually, mRNAs are protected from degradation in cytoplasm by the cap and the poly (A) tail at the 5' and 3' extremities, respectively. However, those mRNAs may suffer a modification by, for example, endonucleases or exonucleases that generate a more fragile region, which will lead to mRNA degradation[76].

Studying the mRNA and the protein expression of the six selected genes (*AGR2, HOXC6, HRK, S100A4, SCML1* and *SPOCK1*), *AGR2* appears to be the most relevant gene for NMIBC development. AGR2 is a member of the protein disulfide isomerase (PDI) family of endoplasmic reticulum-resident proteins with molecular weight of 20 kDa, where it functions as a molecular chaperone in protein folding. Moreover, *AGR2* is usually in the endoplasmic reticulum, but this protein can also be found in the nucleus[77]. *AGR2* may control different aspects of tumor biology, such as, cell cycle, differentiation, migration, invasion and metastasis. *AGR2* was found as a pro-oncogenic protein that attenuate TP53 activity by suppressing

TP53 phosphorylation after DNA damage[78]. Prometastatic characteristics of *AGR2* protein are demonstrated by its interactions with C4.4A and alpha-dystroglycan (DAG-1) – two proteins that play have a role in metastasis formation[79,80]. *AGR2* is overexpressed in a wide variety of tumors formed in different tissues with diverse patterns of genetic alterations, including cancers of the breast[81,82], prostate[83], lung[84] and colorectum[85]. Moreover, *AGR2* also supports aggressive growth and metastasis of a variety of cancer cells[86–88]. A meta-analysis by Tian *et al* reported that *AGR2* overexpression in breast cancer patients was significantly associated with poor survival[89]. Currently, very few studies have centered on AGR2 protein in bladder cancer. Interestingly, Melissa *et al*. recently described that bladder cancer cells secrete AGR2 while normal bladder cells express *AGR2* but do not secrete it[90]. Furthermore, a humanized monoclonal antibody targeting secreted *AGR2* has already been designed, which makes *AGR2* an even more interesting gene to study as a tumor progression/predictive biomarker for patients with NMIBC[91,92].

To test the hypothesis that *AGR2* may be involved in BC progression and aggressiveness, *AGR2* gene was knocked down in BFTC clone cells, which had already suffered a knock-down of the ΔNp63. The knockdown of *AGR2* was performed in both NMIBC, however RT112 cell lines took longer time to grow and it was impossible to perform the experiments in time to present this work. The knock-down of *AGR2* was performed in five different clones and RNA and protein were extracted from each to evaluate which had the lowest level of *AGR2* mRNA and protein, tested also by qRT-PCR, WB and IF assays. The BFTC_A5 was the cell line that showed lower level of *AGR2* mRNA and protein and, because of that, it was used to perform all the functional studies, such as cell cycle, invasion and proliferation assays. Cell cycle assay allowed to analyze the capacity for cell growth by quantifying the amount of DNA inside of a cell. Cell cycle was divided in G1, S, G2 and M phase, in this particularly order. In S phase, the DNA is duplicated and the division of the cell only happened in M phase. DNA was stained with propidium iodide in order to distinguish G2 and G1 phases because, given that if determined cells are dividing faster than others, they should have more number of cells in G2 phase in comparison to G1 phase. BFTC_C showed higher cell growth ratio than BFTC_A5 and BFTC_P which means that when bladder cancer cells do not express ΔNp63 they grow more. Notably, when we knock down *AGR2* gene in these cells, their cell growth decreases. Thus, this methodology allowed confirming the important role of *AGR2* in the control of tumor growth in BFTC cells. To deepen the knowledge of the function of *AGR2* in tumor aggressiveness, proliferation assays were performed, which allowed the quantification of viable cells and to study their capacity to proliferate. Viable cells have the ability to reduce MTS in formazan product, which is soluble in culture media. BFTC_C showed the highest proliferation ratio, followed by BFTC_A5 and BFTC_P cell lines, which suggests that bladder tumor cells that express AGR2 and no ΔNp63 progress more than the ones with low expression of AGR2 and ΔNp63 proteins. Since this study is focused on HG NMIBC which means that they are NMIBC cells with high risk of progression to MIBC, it was important to evaluate the ability of invasion of these knockdown *AGR2* cell lines. Invasion assays showed that BFTC_C displayed a higher invasiveness phenotype followed by BFTC_A5 and BFTC_P. These results suggest that tumor cells with no expression of ΔNp63 have higher ability to invade, however when AGR2 is low, this capacity is lost and the invasiveness decreases.

Overall, tumors with low or no expression of ΔNp63 isoform display higher growth rate and proliferation capacity *in vitro*. Moreover, the absence of this gene showed increase invasiveness ability of the tumor *in vitro*. Furthermore, *in vivo* experiments performed to confirm previous findings, revealed that those cells have higher bladder tumor development and higher metastatic formation. Tumors with low or no expression of ΔNp63 isoform and *AGR2* gene simultaneously showed lower growth rate, lower proliferation

capacity and less invasiveness *in vitro*, comparatively to cells with *AGR2* gene expression. All results considered, *AGR2* gene overexpression may be involved in tumor progression and in an aggressive phenotype. However it is still not known how *AGR2* regulates these features and how this gene interacts with other genes involved in the tumor cell biology.

In accordance with these results, ΔNp63 may inhibit *AGR2* gene by an unknown mechanism and when ΔNp63 is loss, AGR2 protein is up-regulated and has the ability to control cell growth, proliferation and invasion capacities of the tumor. This may be a consequence of AGR2 interaction with other proteins, such as C4.4A and DAG1 proteins that have already been reported in metastasis formation[80,93]. AGR2 is a protein located in the endoplasmic reticulum, however this protein has been already described in the nucleus, where it can regulate TP53 and other transcription factors, such as REPTIN protein[77,94]. REPTIN protein has a role in DNA repair, replication and transcriptional regulation and is overexpressed in various types of cancer, including bladder cancer[95]. It is proposed that ΔNp63 is able to inhibit AGR2 functions and that is one of the reasons why tumors with high ΔNp63 expression do not tend to progress as much as tumors with no or low ΔNp63 expression. Moreover, *SOX2* gene is able to promote *AGR2* function, and since it is found mutated in BFTC cells, this may lead to a higher decrease of *AGR2* in those cells. Furthermore, *AGR2* can act as a *TP53* inhibitor and can also induce cell growth, metastasis and cell migration, interacting with other proteins, such as REPTIN, DAG-1 and C4.4A, among others (**Figure 5.1**).

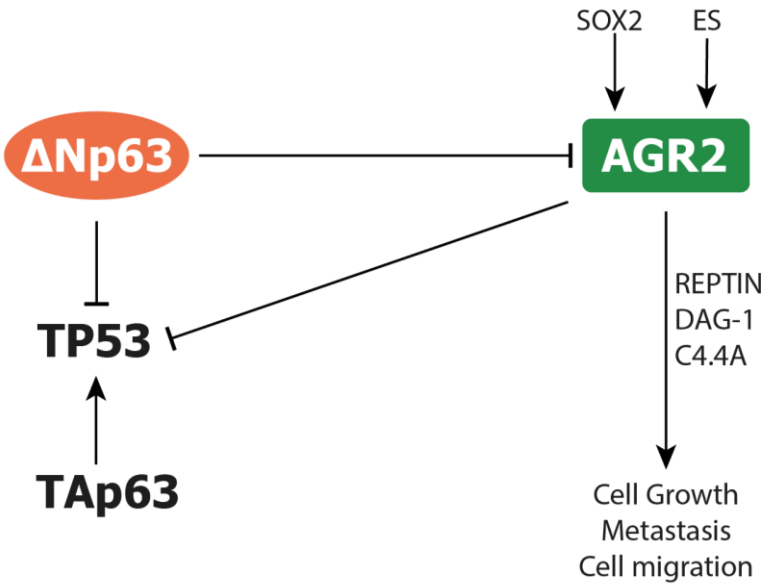

Figure 5.1 Schematic representation of the proposed biological mechanism of *AGR2* regulators and the *AGR2* interactions/functions. ΔNp63, an isoform of *TP63*, is able to inhibit *AGR2* as well *TP53* genes. TAp63, another p63 isoform, has the antagonistic function of ΔNp63 because it can promote transcription of *TP53* gene. *SOX2* gene and Estrogen (ES) are able to promote *AGR2* expression and this protein interacts with other proteins, such as, REPTIN, DAG-1 and C4.4A, among others. These interactions lead to tumor cell growth, metastasis and cell migration.

To the author's knowledge, this is the first study that described ΔNp63, *TP63* isoform, interaction with *AGR2* gene in progression of NMIBC. In this study, bladder tumor cells with no expression of ΔNp63 gene displayed higher proliferation rate whereas those cells with no expression of *AGR2* gene simultaneously, showed lower proliferations rate. These *in vitro* results suggest that *AGR2* may be involved in tumor progression, tumor growth and tumor invasion in bladder cancer, however these experiments must

be repeated to achieve, at least, 3 replicates. The proliferation assay has some technical issues because the number of cells transferred to the 96-well plate was very small and turned it inaccurate. The number of cells is a limiting factor since the well of the 96-well plate is very small and the confluency of the cells should be avoided before the end of the assay. So, for the future, proliferation capacities could be performed with other technique, such as cell trace cell proliferation through flow cytometry. This technique consists in staining the DNA and through subsequent cell divisions, daughter cells receive approximately half of the fluorescent label of their parent cells, allowing the analysis of fluorescence intensities that lead to a determination of the number of generations. Therefore, the number of generations is related with the proliferative capacities of the cells.

To better understand the relevance of *AGR2* gene in bladder cancer progression, *in vivo* studies will be performed. Moreover, to confirm the findings in another setting, the same studies performed for BFTC cell line will be done for RT112 cell line. Henceforth, immunofluorescence of *AGR2* expression in T1 NMIBC human specimen in tissue microarrays (TMA) will be performed to validate the *in vitro* and *in vivo* results, and to test whether *AGR2* is a prognostic biomarker in this clinical setting. TMAs are used in the pathology clinical setting to molecularly characterize tumors in a simple and cost-effective manner. TMA studies will allow correlating *AGR2* expression level with patient's conditions, such as, prognosis, risk of progression, metastasis, time of survival, etc. Also, mechanistic studies will be important to elucidate how *AGR2* induces the aggressiveness phenotype to clarify our hypothesis displayed in **Figure 5.1**.

Afterwards, if *AGR2* is a good factor of NMIBC progression, patients whose tumors are characterized by high levels of AGR2 protein may be treated with a humanized monoclonal antibody and followed by observation, in case of benefiting from this novel treatment. The development of a clinical trial to test this new therapeutic approach, if positive, could render a great alternative for patients for whom only radical cystectomy is currently available. Overall, in this work, *AGR2* is described as a potential factor for progression of NMIBC to MIBC. *AGR2* gene is important in tumor development and it can be a biomarker to distinguish the tumors that should (or not) undergo to a more invasive treatment. For example, cystectomy may be beneficial for clinically high-risk patients with a high progression score, while continued surveillance, BCG instillations and/or anti-*AGR2* treatment may be beneficial for clinically high-risk patients with low progression score. Patients with low clinical risk but high progression scores may be monitored as clinically high-risk patients[52].

In the future, it would also be interesting to do the same type of analyses with the *S100A4* gene given it also has showed higher gene level, higher mRNA level and higher protein level in clones ($\Delta Np63^-$) than in parental ($\Delta Np63^+$) cells in BFTC cell line, and it is a well-known gene involved in tumor progression, never previously studied in NMIBC.

6 Conclusion

NMIBC is a heterogeneous disease that includes tumors with high risk and low risk of tumor progression. Nowadays, using clinic-pathological features alone it is difficult to differentiate amongst these tumors and sometimes the oncologic patients suffers an overtreatment, mainly because the clinicians do not have the adequate tools to identify the high risk tumor that needs this radical treatment. Accordingly, the discovery of progression biomarkers is essential to decrease the overtreatment and to increase the quality of life of each patient depending on the type of tumor developed.

ΔNp63, isoform of *TP63* gene, has been studied as a protective factor of NMIBC progression because when this isoform is down-regulated tumors have higher risk of progression, higher invasive capacities and higher metastasis formation. The main goal of this work was to discover the genetic alterations associated with ΔNp63 isoform loss that confers the aggressiveness phenotype of tumor cells. Interestingly, when ΔNp63 is down-regulated *AGR2* gene is up-regulated and, in this report, the *AGR2* gene was identified as a potential factor of progression of NMIBC. The functional analyses performed after knock down of *AGR2* confirmed the implication of *AGR2* in tumor aggressiveness, given that cells with low expression of *AGR2* showed lower proliferation rate and invasive capacities, as well as lower cell division, *in vitro*. However, more studies are needed to validate this hypothesis, such as *in vivo* tumorigenesis and metastasis assays and immunofluorescence analyses of AGR2 protein in T1 NMIBC patient samples tissues microarrays (TMA) that will enable to transfer these findings to a new level of scientific evidence.

This work is the first to address the interaction between *AGR2* and ΔNp63 and its role in tumor progression, allowing a better understanding of the mechanisms of BC progression. These results could help, in the future, to distinguish the low risk from the high risk tumors and could help clinicians to determine how patients with HG NMIBC should be treated, depending on their tumor molecular characteristics. Moreover, the existence of a humanized antibody against *AGR2* could open the opportunity of performing clinical trials to test this novel therapeutic method for high risk T1 NMIBC, allowing a more conservative approach, thus improving patients' quality of life.

7 References

1. Ferlay, J. *et al.* Cancer incidence and mortality worldwide: Sources, methods and major patterns in GLOBOCAN 2012. *Int. J. Cancer* **136,** E359–E386 (2015).

2. Antoni, S. *et al.* Bladder cancer incidence and mortality: A global overview and recent trends. *Eur. Urol.* **71,** 96–108 (2016).

3. Ferlay, J. *et al.* Cancer incidence and mortality patterns in Europe: Estimates for 40 countries in 2012. *Eur. J. Cancer* **49,** 1374–1403 (2013).

4. Gui, Y. *et al.* Frequent mutations of chromatin remodeling genes in transitional cell carcinoma of the bladder. *Nat. Genet.* **43,** 875–878 (2011).

5. Di Pierro, G. B. *et al.* Bladder cancer: a simple model becomes complex. *Curr. Genomics* **13,** 395–415 (2012).

6. Lamm, D. *et al.* Defining progression in nonmuscle invasive bladder cancer: it is time for a new, standard definition. *J. Urol.* **191,** 20–7 (2014).

7. Orsola, A., Palou, J. & Solsona, E. High-risk nonmuscle invasive bladder cancer. *Hematol. Oncol. Clin. North Am.* **29,** 227–236 (2015).

8. McConkey, D. J. *et al.* Molecular genetics of bladder cancer: Emerging mechanisms of tumor initiation and progression. *Urol. Oncol. Semin. Orig. Investig.* **28,** 429–440 (2010).

9. Czerniak, B., Dinney, C. & McConkey, D. Origins of bladder cancer. *Annu. Rev. Pathol.* 149–174 (2016). doi:10.1146/annurev-pathol-012513-104703

10. Kulkarni, G. S. *et al.* An updated critical analysis of the treatment strategy for newly diagnosed high-grade T1 (Previously T1G3) bladder cancer. *Eur. Urol.* **57,** 60–70 (2010).

11. Cheng, L. *et al.* Survival of patients with carcinoma in situ of the urinary bladder. *Cancer* **85,** 2469–74 (1999).

12. Sylvester, R. J. *et al.* Predicting recurrence and progression in individual patients with stage Ta T1 bladder cancer using EORTC risk tables: A combined analysis of 2596 patients from seven EORTC trials. *Eur. Urol.* **49,** 466–475 (2006).

13. Hanahan, D. & Weinberg, R. A. Hallmarks of cancer: The next generation. *Cell* **144,** 646–674 (2011).

14. Wu, X.-R. Urothelial tumorigenesis: a tale of divergent pathways. *Nat. Rev. Cancer* **5,** 713–25 (2005).

15. Billerey, C. *et al.* Frequent FGFR3 mutations in papillary non-invasive bladder (pTa) tumors. *Am. J. Pathol.* **158,** 1955–9 (2001).

16. Sfakianos, J. P. *et al.* The role of PTEN tumor suppressor pathway staining in carcinoma in situ of the bladder. *Urol. Oncol. Semin. Orig. Investig.* **32,** 657–662 (2014).

17. Knowles, M. A., Platt, F. M., Ross, R. L. & Hurst, C. D. Phosphatidylinositol 3-kinase (PI3K) pathway activation in bladder cancer. *Cancer Metastasis Rev.* **28,** 305–316 (2009).

18. Traczyk, M. *et al.* Polymorphic variants of H-RAS protooncogene and their possible role in bladder cancer etiology. *Cent. Eur. J. Urol.* **65,** 84–87 (2012).

19. Castillo-Martin, M., Domingo-Domenech, J., Karni-Schmidt, O., Matos, T. & Cordon-Cardo, C. Molecular pathways of urothelial development and bladder tumorigenesis. *Urologic Oncology: Seminars and Original Investigations* (2010). doi:10.1016/j.urolonc.2009.04.019

20. Shen, H. *et al.* 6p22.3 amplification as a biomarker and potential therapeutic target of advanced stage bladder cancer. *Oncotarget* **4,** 2124–2134 (2013).

21. Kram, a *et al.* Mapping and genome sequence analysis of chromosome 5 regions involved in bladder cancer

progression. *Lab. Invest.* **81,** 1039–48 (2001).

22. Cai, T. *et al.* Loss of heterozygosis on chromosome 18q21-23 and muscle-invasive bladder cancer natural history. *Oncol. Lett.* **10,** 2569–2573 (2015).

23. Zieger, K., Wiuf, C., Jensen, K. M.-E., Ørntoft, T. F. & Dyrskjøt, L. Chromosomal imbalance in the progression of high-risk non-muscle invasive bladder cancer. *BMC Cancer* **9,** 149 (2009).

24. Zieger, K., Marcussen, N., Borre, M., Ørntoft, T. F. & Dyrskjøt, L. Consistent genomic alterations in carcinoma in situ of the urinary bladder confirm the presence of two major pathways in bladder cancer development. *Int. J. Cancer* **125,** 2095–2103 (2009).

25. Choi, W. *et al.* Identification of distinct basal and luminal subtypes of muscle-invasive bladder cancer with different sensitivities to frontline chemotherapy. *Cancer Cell* **25,** 152–165 (2014).

26. Dadhania, V. *et al.* Meta-analysis of the luminal and basal subtypes of bladder cancer and the identification of signature immunohistochemical markers for clinical use. *EbioMedicine* (2016).

27. Sexton, W. J. *et al.* Bladder cancer: a review of non-muscle invasive disease. *Cancer Control* **17,** 256–268 (2010).

28. Iii, C. H. S. *et al.* Distinct pattern of p53 mutations in bladder cancer : relationship to tobacco usage distinct pattern of p53 mutations in bladder cancer : relationship to tobacco. *Cancer Res.* **53,** 1162–1166 (1993).

29. Letašiová, S. *et al.* Bladder cancer, a review of the environmental risk factors. *Environ. Heal.* **11 Suppl 1,** S11 (2012).

30. Mendez, W. M. *et al.* Relationships between arsenic concentrations in drinking water and lung and bladder cancer incidence in U.S. counties. *J. Expo. Sci. Environ. Epidemiol.* 1–9 (2016).

31. Lewis, J. D. *et al.* Risk of bladder cancer among diabetic patients treated with pioglitazone: Interim report of a longitudinal cohort study. *Diabetes Care* **34,** 916–922 (2011).

32. Mostafa, M. H. & Sheweita, S. a. Relationship between schistosomiasis and bladder cancer evidence supporting the relationship between schistosomiasis and bladder. *Clin. Microbiol. Rev.* **12,** 97–111 (1999).

33. Hemminki, K., Bermejo, J. L., Ji, J. & Kumar, R. Familial bladder cancer and the related genes. *Curr. Opin. Urol.* **21,** 386–92 (2011).

34. Murta-Nascimento, C. *et al.* Risk of bladder cancer associated with family history of cancer: do low-penetrance polymorphisms account for the increase in risk? *Cancer Epidemiol. Biomarkers Prev.* **16,** 1595–1600 (2007).

35. Marks, P. *et al.* Female with bladder cancer: what and why is there a difference? *Transl. Androl. Urol.* **5,** 668–682 (2016).

36. Gaya, J. M. *et al.* DeltaNp63 expression is a protective factor of progression in clinical high grade T1 bladder cancer. *J. Urol.* **193,** 1144–1150 (2015).

37. Urist, M. J. *et al.* Loss of p63 expression is associated with tumor progression in bladder cancer. *Am. J. Pathol.* **161,** 1199–206 (2002).

38. Gonfloni, S., Caputo, V. & Iannizzotto, V. P63 in health and cancer. *Int. J. Dev. Biol.* **59,** 87–93 (2015).

39. Park, B. J. *et al.* Frequent alteration of p63 expression in human primary bladder carcinomas. *Cancer Res.* **60,** 3370–3374 (2000).

40. Di Como, C. J. *et al.* P63 expression profiles in human normal and tumor tissues. *Clin. Cancer Res.* **8,** 494–501 (2002).

41. Flores, E. R. *et al.* Tumor predisposition in mice mutant for p63 and p73: Evidence for broader tumor suppressor functions for the p53 family. *Cancer Cell* **7,** 363–373 (2005).

42. Buckley, N. E. *et al.* The DeltaNp63 proteins are key allies of BRCA1 in the prevention of basal-like breast cancer. *Cancer Res.* **71,** 1933–1944 (2011).

43. Karni-Schmidt, O. *et al.* Distinct expression profiles of p63 variants during urothelial development and bladder cancer progression. *Am. J. Pathol.* **178,** 1350–1360 (2011).

44. Bergholz, J. & Xiao, Z. X. Role of p63 in development, tumorigenesis and cancer progression. *Cancer Microenviron.* 1–12 (2012).

45. Melino, G. P63 is a suppressor of tumorigenesis and metastasis interacting with mutant p53. *Cell Death Differ.* **18,** 1487–1499 (2011).

46. Kamat, A. M., Bagcioglu, M. & Huri, E. What is new in non-muscle-invasive bladder cancer in 2016? *Turkish J. Urol.* **43,** 9–13 (2017).

47. Bochner, B. H. Bladder cancer. *Nat. Publ. Gr.* 1–2 (2011).

48. Manikandan, R., Rodriguez, O. & Redorta, J. P. Nonmuscle-invasive bladder cancer: what's changing and what has changed. *Urology* **84,** 1–8 (2017).

49. Bellmunt, J. *et al.* Bladder cancer: ESMO practice guidelines for diagnosis, treatment and follow-up. *Ann. Oncol.* **25,** iii40-iii48 (2014).

50. Susman, E. New NCCN bladder cancer guidelines add maintenance BCG. *Oncol. Times* (2015).

51. Van Rhijn, B. W. G. *et al.* The FGFR3 mutation is related to favorable pT1 bladder cancer. *J. Urol.* **187,** 310–314 (2012).

52. Dyrskjøt, L. *et al.* Prognostic impact of a 12-gene progression score in mon – muscle invasive bladder Cancer : A prospective multicentre alidation study. 1–9 (2017).

53. Karam, J. A. *et al.* Use of combined apoptosis biomarkers for prediction of bladder cancer recurrence and mortality after radical cystectomy. *Lancet Oncol.* **8,** 128–136 (2007).

54. Serruys, P. W. *et al.* Accumulation of nuclear p53 and tumor progression in bladder cancer. *N. Engl. J. Med.* **331,** 481 (1994).

55. Lindgren, D. *et al.* Integrated genomic and gene expression profiling identifies two major genomic circuits in urothelial carcinoma. *PLoS One* **7,** 1–11 (2012).

56. Pietzak, E. J. *et al.* Next-generation sequencing of nonmuscle invasive bladder cancer reveals potential biomarkers and rational therapeutic targets. *Eur. Urol.* 1–8 (2017).

57. Isharwal, S. *et al.* Prognostic value of TERT alterations and mutational and copy number alteration burden in urothelial carcinoma. *Eur. Urol. Focus* 2–5 (2017).

58. Niegisch, G. & Albers, P. Which patients benefit the most from neoadjuvant chemotherapy in advanced bladder cancer? *Curr. Opin. Urol.* **21,** 434–9 (2011).

59. Qiagen. Isolation of endotoxin-free plasmid DNA using the Qiagen Plasmid Midi Kit. *Qiagen Suppl. Protoc.* 1–3 (2001).

60. Reis, L. O. *et al.* Anatomical features of the urethra and urinary bladder catheterization in female mice and rats. An essential translational tool. *Acta Cirúrgica Bras.* **26,** 106–110 (2011).

61. Karni-Schmidt, O. *et al.* Distinct expression profiles of p63 variants during urothelial development and bladder cancer progression. *Am. J. Pathol.* **178,** 1350–1360 (2011).

62. Morey, J. S., Ryan, J. C. & Van Dolah, F. M. Microarray validation: factors influencing correlation between oligonucleotide microarrays and real-time PCR. *Biol. Proced. Online* **8,** 175–93 (2006).

63. Vogiatzi, F. *et al.* Mutant p53 promotes tumor progression and metastasis by the endoplasmic reticulum

UDPase ENTPD5. *Proc. Natl. Acad. Sci.* **113,** E8433–E8442 (2016).

64. Petitjean, A., Achatz, M. I. W., Borresen-Dale, A. L., Hainaut, P. & Olivier, M. TP53 mutations in human cancers: functional selection and impact on cancer prognosis and outcomes. *Oncogene* **26,** 2157–2165 (2007).

65. McCubrey, J. A. *et al.* Roles of TP53 in determining therapeutic sensitivity, growth, cellular senescence, invasion and metastasis. *Adv. Biol. Regul.* **63,** 32–48 (2017).

66. Sacristan, R. *et al.* Molecular classification of non-muscle-invasive bladder cancer (pTa Low-Grade, pT1 Low-Grade, and pT1 High-Grade Subgroups) using methylation of tumor-suppressor genes. *J. Mol. Diagnostics* **16,** 564–572 (2014).

67. Sarkis, A. S. *et al.* Nuclear overexpression of p53 protein in transitional cell ladder carcinoma : A marker for disease progression background. *J. Natl. Cancer Inst.* **85,** 53–59 (1993).

68. Song, X. *et al.* Targeting mTOR and p53 signaling inhibits muscle invasive bladder cancer in vivo. *Cancer Prev Res* **55,** 237–246 (2017).

69. Singh, R. R. *et al.* Clinical massively parallel next-generation sequencing analysis of 409 cancer-related genes for mutations and copy number variations in solid tumours. *Br. J. Cancer* **111,** 2014–2023 (2014).

70. Wu and Roberts. ARID1A mutations in cancer: Another epigenetic tumor supressor? *Cancer Discov.* **3,** 35–43 (2013).

71. Nottingham, C. U., Patel, S. G., Clark, P. E., Degraff, D. J. & Gregg, J. R. Clinics in oncology SOX2 expression in patients who underwent radical cystectomy for urothelial carcinoma of the bladder. **1,** 1–6 (2016).

72. Wu, C.-C., Chiu, Y.-F., Chou, Y.-T. & Wang, Y.-H. Abstract 3408: Oncogenic SOX2 signaling in bladder cancer. *Cancer Res.* **76,** 3408 LP-3408 (2016).

73. Knowles, M. A. & Hurst, C. D. Molecular biology of bladder cancer: new insights into pathogenesis and clinical diversity. *Nat. Rev. Cancer* **15,** 25–41 (2015).

74. Abdulamir, A. S., Hafidh, R. R., Kadhim, H. S. & Abubakar, F. Tumor markers of bladder cancer: the schistosomal bladder tumors versus non-schistosomal bladder tumors. *J. Exp. Clin. Cancer Res.* **28,** 27 (2009).

75. Dueñas, M. *et al.* PIK3CA gene alterations in bladder cancer are frequent and associate with reduced recurrence in non-muscle invasive tumors. *Mol. Carcinog.* **54,** 566–576 (2015).

76. Tourrière, H., Chebli, K. & Tazi, J. mRNA degradation machines in eukaryotic cells. *Biochimie* **84,** 821–837 (2002).

77. Maslon, M. M., Hrstka, R., Vojtesek, B. & Hupp, T. R. A divergent substrate-binding loop within the pro-oncogenic protein anterior gradient-2 forms a docking site for reptin. *J. Mol. Biol.* **404,** 418–438 (2010).

78. Pohler, E. *et al.* The Barrett's antigen anterior gradient-2 silences the p53 transcriptional response to DNA damage. *Mol Cell Proteomics* **3,** 534–547 (2004).

79. Brychtova, V., Vojtesek, B. & Hrstka, R. Anterior gradient 2: A novel player in tumor cell biology. *Cancer Lett.* **304,** 1–7 (2011).

80. Arumugam, T. *et al.* New blocking antibodies against novel AGR2-C4. 4A pathway reduce growth and metastasis of pancreatic tumors and increase survival in mice. *Mol Cancer Ther* **14,** (2015).

81. Salmans, M. L., Zhao, F. & Andersen, B. The estrogen-regulated anterior gradient 2 (AGR2) protein in breast cancer: a potential drug target and biomarker. *Breast Cancer Res.* **15,** 204 (2013).

82. Hrstka, R., Nenutil, R. & Bouchal, P. Targeted proteomics driven verification of biomarker candidates associated with breast cancer aggressiveness. *BBA - Proteins Proteomics* (2017).

83. Kani, K. *et al.* Anterior gradient 2 (AGR2): blood-based biomarker elevated in metastatic prostate cancer associated with the neuroendocrine phenotype. *Prostate* **2,** (2012).

84. Zhu, H. *et al.* High resolution analysis of genomic aberrations by metaphase and array comparative genomic hybridization identifies candidate tumour genes in lung cancer cell lines. *Cancer Lett.* **245,** 303–314 (2007).

85. Gao, H. *et al.* Anterior gradient 2 : A new target to treat colorectal cancer. *Med. Hypotheses* **80,** 706–708 (2013).

86. Chevet, E. *et al.* Emerging roles for the pro-oncogenic anterior gradient-2 in cancer development. *Oncogene* **32,** 2499–2509 (2013).

87. Fessart, D. *et al.* Secretion of protein disulphide isomerase AGR2 confers tumorigenic properties. *Cancer Biol. Cell Biol.* **5,** 1–24 (2016).

88. Barraclough, D. L. *et al.* The metastasis-associated anterior gradient 2 protein is correlated with poor survival of breast cancer patients. *Am. J. Pathol.* **175,** 1848–1857 (2009).

89. Tian, S. *et al.* The prognostic value of AGR2 expression in solid tumours: a systematic review and meta-analysis. *Sci. Rep.* **7,** 15500 (2017).

90. Ho, M. E. *et al.* Bladder cancer cells secrete while normal bladder cells express but do not secrete AGR2. *Oncotarget* **7,** 15747–15756 (2016).

91. Guo, H. *et al.* A humanized monoclonal antibody targeting secreted anterior gradient 2 effectively inhibits the xenograft tumor growth. *Biochem. Biophys. Res. Commun.* **475,** 57–63 (2016).

92. Li, D., Wu, Z., Guo, H., Zhu, Q. & Mashausi, D. S. AGR2 blocking antibody and use thereof. (2017).

93. Fletcher, G. C. *et al.* hAG-2 and hAG-3, human homologues of genes involved in differentiation, are associated with oestrogen receptor-positive breast tumours and interact with metastasis gene C4.4a and dystroglycan. *Br. J. Cancer* **88,** 579–585 (2003).

94. Orzol, P. Molecular complexity of p63 in cancer. (2016).

95. Grigoletto, A., Lestienne, P. & Rosenbaum, J. The multifaceted proteins Reptin and Pontin as major players in cancer. *Biochim. Biophys. Acta - Rev. Cancer* **1815,** 147–157 (2011).

8 Supplementary Data

Table 8.1 Sequences of the primers used to perform qRT-PCR.

Gene		Sequence	Ref.
GAPDH	F	5'-CAGCCTCAAGATCATCAGCA-3'	18932030
	R	5'-GTCTTCTGGGTGGCAGTGAT-3'	
ΔNP63	F	5'-TGCCCAGACTCAATTTAGTGAG-3'	20600197
	R	5'-TCTGGATGGGGCATGTCTTTGC-3'	
CHD2	F	5'-GAGAATGCAAGGCCCTGAAGC-3'	10336022
	R	5'-CCAGAAACAGTAAGGAAAATTGCAC-3'	
HOXC6	F	5'-ATGAATTCGCACAGTGGGGTC-3'	10336022
	R	5'-GGTACCGCGAGTAGATCTGG-3'	
HRK	F	5'-GGCGGAACTTGTAGGAACGC-3'	10336022
	R	5'-TTTTCACCAACCTGTTGCTCGC-3'	
S100A4	F	5'-TCTTGGTTTGATCCTGACTGC-3'	10336022
	R	5'-GCCCGAGTACTTGTGGAAGG-3'	
AGR2	F	5'-TTGGGGAAAGGAAGGTTCG-3'	10336022
	R	5'-CTCCATGGCAACTCGGATTTC-3'	
EPDR1	F	5'-GCTGATCCCCTGCAAGAGATTATTT-3'	10336022
	R	5'-GGCTGTGTCAGGGTCATCTT-3'	
SCML1	F	5'-CAGGCTCTGTCACTAAAATAGGAAC-3'	10336022
	R	5'-GATCTCGCATGGAAACGTTGG-3'	
SPOCK1	F	5'-GCTCAGATGGCCACTCCTAC-3'	10336022
	R	5'-TCTGTGCAGGCACTCCTTTC-3'	

Table 8.2 Summary of the antibodies and its respective characteristics.

Gene	anti-	Clone	# Catalog	Company	Dilution		Molecular Weight (kDa)
					WB	IF	
AGR2	rabbit	monoclonal	ab76473	Abcam	1:2000	1:100	20
HOXC6	mouse	monoclonal	sc-376330	Santa Cruz Biotechnology	1:500	1:50	27
HRK	rabbit	polyclonal	ab45419	Abcam	-	1:100	10
S100A4	rabbit	monoclonal	13018	Cell Signaling	1:1000	1:50	12
SCML1	mouse	monoclonal	sc-135622	Santa Cruz Biotechnology	1:200	1:50	37
β-actin	mouse	monoclonal	MA1-91399	Thermo Fisher Scientific	1:10000	-	42

Table 8.3 Summary of volume of protein and reagents to perform the protein running assay.

Average Protein Concentration	Supernatant volume (40-50 µg)	RIPA buffer	Laemnie dye (4X)	Total Volume
N µg/µL	(40/**N**) = *x* µL	22,5 – *x* µL	7,5 µL	30 µL

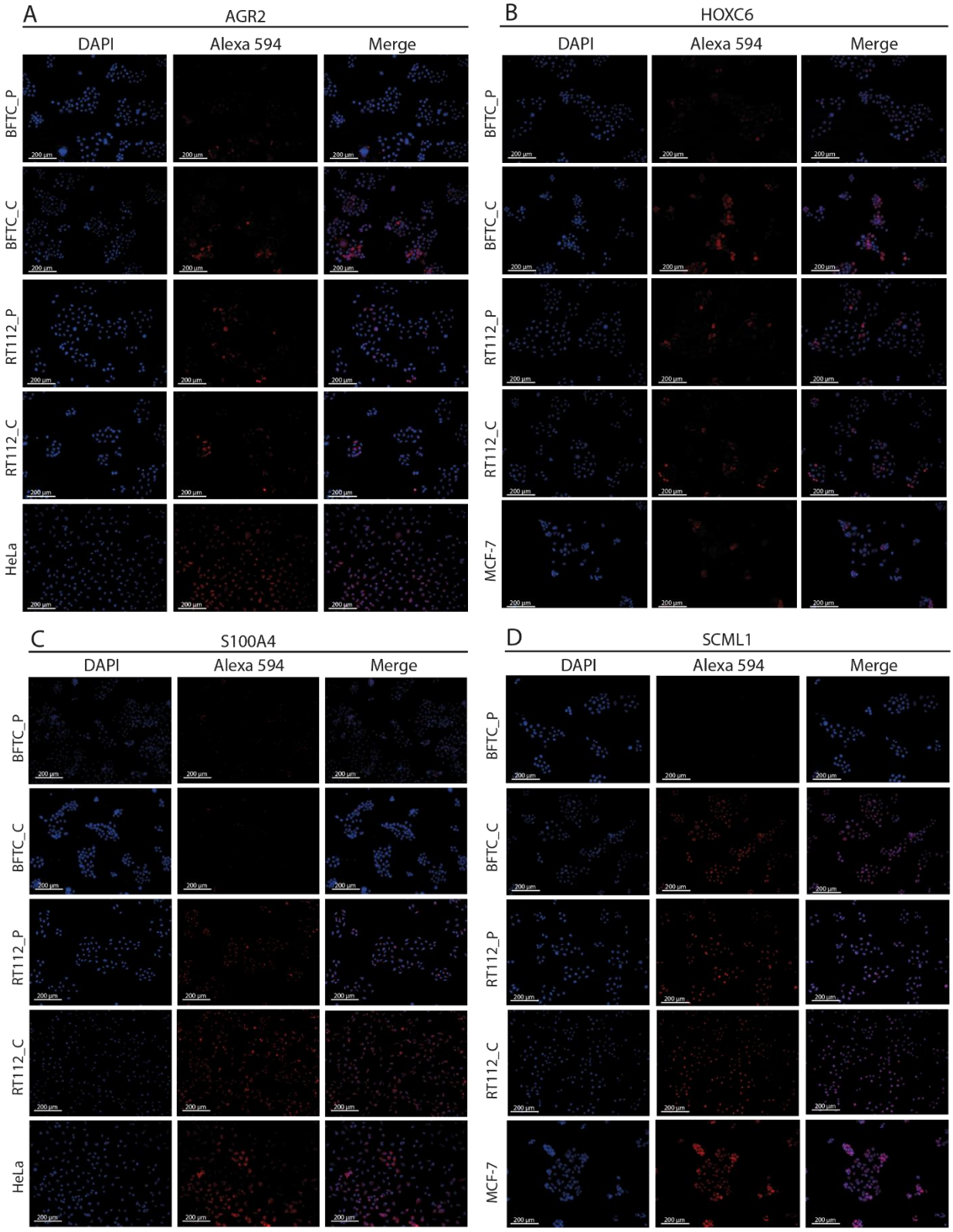

Figure 8.1 Immunofluorescence of AGR2, HOXC6, S100A4 and SCML1 proteins in BFTC_C, BFTC_P, RT112_C, RTT12_P and control positive cell lines.

Figure 8.1 Immunofluorescence of AGR2, HOXC6, S100A4 and SCML1 proteins in BFTC_C, BFTC_P, RT112_C, RTT12_P and control positive cell lines. **A:** Representative immunofluorescence using anti-AGR2 antibody in BFTC_L_C, BFTC_L_P, RT112_L_C, RT112_L_P cells and HeLa cells as positive control. **B:** Representative immunofluorescence using anti-HOXC6 antibody on BFTC_L_C, BFTC_L_P, RT112_L_C, RT112_L_P cells and MCF-7 cells as positive control. **C:** Representative immunofluorescence using anti-S100A4 antibody on BFTC_L_C, BFTC_L_P, RT112_L_C, RT112_L_P cells and HeLa cells as positive control. **D:** Representative immunofluorescence using anti-SCML1 antibody on BFTC_L_C, BFTC_L_P, RT112_L_C, RT112_L_P cells and MCF-7 cells as positive control.

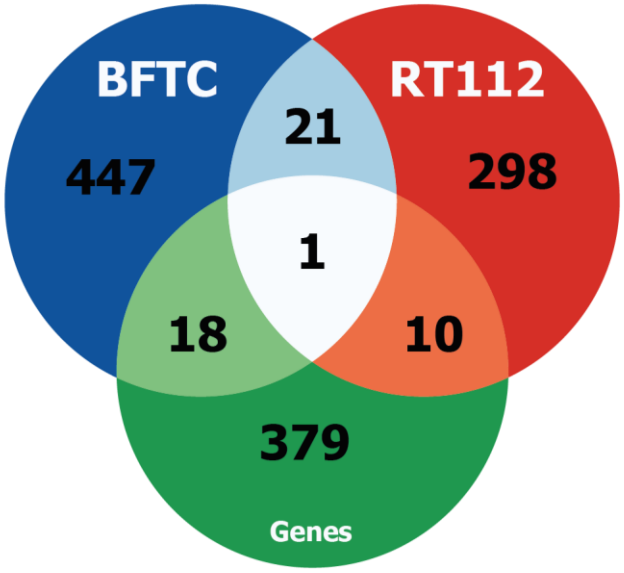

Figure 8.2 Venn diagram of BFTC and RT112 mutated genes and their relevance in tumor biology. A panel of mutated genes described in BFTC and RT112 cell lines were compared with a panel of important genes in tumor biology described by IonTorrent[69]. 18 out of the 487 mutated genes of the BFTC were in common with 409 panel of the important genes and they are *BAI3*, *BCL9*, *PKHD1*, *NRAS*, *BLM*, *TNK2*, *CDH11*, *PTCH1*, *ARID2*, *CDH20*, *TRRAP*, *SRC*, *ITGA9*, *FOXP1*, *SAMD9*, *DCC*, *CSF1R* and *SOX2* genes. 10 out of the 330 mutated genes of RT112 cell line were in common with 409 panel of the important genes and they are *KDM6A*, *EPHA7*, *NF1*, *MYC*, *PRDM1*, *FLCN*, *PI3KCA*, *HSP90AB1*, *CEBPA* and *HCAR1* genes. BFTC and RT112 cell lines showed 22 common mutated genes, *ESX1*, *NOS1*, *TENM4*, *APOB*, *ADAMTS2*, *AHNAK*, *TEMEM209*, *KIAA1551*, *KANSL1*, *NACA*, *MUC4*, *IBSP FAM83A*, *TRIM66*, *RYR2*, *ZNF853*, *MT-ND5*, *PRR12*, *KMT2C* and *PAPOLB*, but only one was in common with the panel of the important genes that are *TP53* gene.